CHAPETER-III RESULTS

An attempt was made in the present study to estimate NPP of deciduous forest covers of KNP, BNP and MNP using field based measurements and satellite data driven CASA ecosystem model, for the period 2010-2014. Knowledge of statistical tools and GIS were applied to achieve the desired objectives in the study. The resultant outputs are described here.

3.1 Kanha National Park

3.1.1 Field inventory: Among the ten tropical deciduous forest sites studied in KNP, there were 767 trees recorded in 10 quadrates each of 0.1 ha, whose DBH was ≥ 3.18 cm and represented by 54 tree species. Plot-wise distribution of tree types with their percentage contribution to the total tree population is presented in **Appendix 3**. Of the 54 species, nine species indicated stand density of >2%, whereas 45 species showed stand density of ≤ 2% of the total tree population. Out of all the tree species, Sal (*Shorea robusta*) was found to be maximum with the presence of 381 trees, which was estimated to be 49.64% of the measured tree density (767 trees). Descriptive statistics of the sample plots studied in KNP is presented in **Table 6**. Amongst all the sample plots, one of the sites in Kanha (Plot-9) contained the greatest stand density of 157 trees, while another site in Kanha (Plot-8) witnessed the lowest tree density with 18 trees.

Table 6: *Descriptive statistics of different sample plots in KNP (Values are mean and standard deviation of five years observations).*

Location	Plot	Tree density/0.1 ha	Average tree height (m) ±SD	Average DBH (cm)±SD
Mukki	1	42	22.31±4.20	24.5±0.48
Supkhar	2	93	19.37±6.57	21.6±0.28
Supkhar	3	90	13.81±7.20	20.8±0.31
Bhaisanghat	4	67	8.14±3.58	17.4±0.56
Bhaisanghat	5	62	11.74±5.68	19.9±0.36
Kisli	6	23	25.17±7.11	37.6±0.56
Kisli	7	100	11.88±4.17	17.1±0.25
Kanha	8	18	24.88±5.54	49±0.4
Kanha	9	157	11.85±10.53	13.2±0.4
Sarhi	10	115	8.46±3.9	12.5±0.55

The tallest trees were found in Plot-6 with an average height of 25.17±7.11m, while shortest trees were observed for Plot-4 with an average height of 8.14±3.9m. Substantial variation in DBH of trees was noticed among the sample plots. It was found to be more

in plot-8 with a mean of 49.0±0.4cm in contrast to the plot-10 (12.5±0.55cm), followed by Plot-9 (13.2±0.4cm).

Aboveground biomass (AGB): AGB was estimated using volumetric regression equations for the trees having DBH ≥ 3.18 cm. AGB estimation was carried out for each tree species of different classes in each sample plot for the period 2010-2014. Per plot biomass (0.1ha) was determined by summing up the biomass of different individuals occurring in each plot. After calculating per plot AGB (kg/0.1ha), the total biomass was calculated in megagrams per hectare (Mg ha^{-1}), and these values were extrapolated to the hectare using Eq.2. Plot-wise biomass per hectare for the period 2010-2014 is presented **Table 7**. A wide range of AGB was occurred between plots with 170.9 Mg ha^{-1} to 482.1 Mg ha^{-1}. Plot-2 holds the greatest biomass throughout the study period with an average biomass of 471.4±10.8 Mg ha^{-1}, ranging from 455 Mg ha^{-1} (2011) to 482.1 Mg ha^{-1} (2014). Though Plot-2 had relatively less tree density (93 trees/0.1 ha), high biomass can be justified because of the occurrence of huge *Shorea robusta* trees with an average height of 19m and mean DBH of 21.6cm.

Table 7: *AGB for different sample plots in KNP for the period 2010-2014.*

		AGB (Mg ha^{-1})					
Location	Plot	2010	2011	2012	2013	2014	Mean±SD
Mukki	1	280.5	290.8	301.5	298.8	303.9	295.1±9.54
Supkhar	2	455.0	466.3	476.7	476.7	482.1	471.4±10.8
Supkhar	3	405.4	417.3	427.2	427.6	434.0	422.3±11.19
Bhaisanghat	4	178.5	190.5	199.1	197.1	207.7	194.6±10.92
Bhaisanghat	5	346.9	353.7	361.9	360.0	365.7	357.6±7.41
Kisli	6	375.8	388.8	394.4	400.0	398.6	391.5±9.79
Kisli	7	253.0	258.4	268.5	266.4	272.8	263.8±8.0
Kanha	8	435.5	444.1	453.2	450.8	453.0	447.3±7.58
Kanha	9	265.7	274.8	288.6	287.7	300.0	283.4±13.33
Sarhi	10	170.9	183.1	196.7	193.8	201.3	189.2±12.19

Least biomass storage was accounted throughout the study period in Plot-10 with an average biomass of 189.2±12.19 Mg ha^{-1}, varying from 170.9 Mg ha^{-1} (2011) to 2013 Mg ha^{-1} (2014). Mean AGB across the plots was found to be highest in 2014 (341.91±100 Mg ha^{-1}), whereas the lowest AGB (316.71±102 Mg ha^{-1}) was observed in 2010. This inter-annual variation in AGB was attributed to variation in DBH, tree density, and percentage of trees showed increment in their growth. Inter-annual

variation in these tree related attributes are presented in **Appendix 4**. Of the 10 plots, 100% of trees in Plot-4, while only 85% of the trees in Plot-7 were indicated increment in their growth (DBH), which were the highest and lowest among all the plots. About 91%-99% of trees in the remaining plots were exhibited increment in their growth. All trees (100%) across the plots showed increment in 2012, whereas only 91% of trees indicated increment in 2011. Increment in DBH was another crucial biophysical parameter, where wide variation in AGB was observed across the plots due its variation. Increment in DBH was comparatively higher in mixed forest (Plot-6, Plot-10, and Plot-4) rather than in the forest dominated by single species, i.e., *Shorea robusta* (Plot-2, Plot-3, Plot-8 and Plot-9). Plots those covered with mixed forest species indicated increment in the range of 0.48cm $year^{-1}$ (Plot-10) to 0.53cm $year^{-1}$ (Plot-6). Whereas *Shorea robusta* dominated plots showed increment between 0.25cm $year^{-1}$ (Plot-2) and 0.36cm $year^{-1}$ (Plot-8). Plot-7 showed the lowest increment among all the plots with 0.21cm $year^{-1}$. Though only 91% of trees across the plots showed increment in 2011, but mean increment in DBH was found to be highest in 2011 with 0.48cm $year^{-1}$, while the lowest increment was observed in 2014 with an average of 0.26cm $year^{-1}$. Percentage change (RD) in AGB across the study years is presented in **Appendix 5**. RD in AGB represented as $RD(\%)=100*((AGB_i-AGB_{2010})/AGB_{2010})$, where i represent AGB in 2011, 2012, 2013 and 2014, respectively. RD across the plot was found to be highest in 2014 with an average of 9.17%. Whereas the lowest change in AGB was observed in 2011 with a mean of 3.59%. Mean change in AGB across the study period was maximum at Plot-10 (13.36%), whereas minimum change in AGB was observed in Plot-8 (3.39%).

Field based NPP : Net primary productivity (NPP) of the tree species lying within the sample plots was estimated by dividing change in their AGB (ΔAGB) with time difference (Δt). More specifically, ΔAGB is the difference between current AGB (t2) and the back calculated AGB (t1). NPP value thus obtained was kg/0.1ha/year. After calculating NPP per plot, total NPP was calculated in megagrams per hectare per year (Mg ha^{-1} $year^{-1}$) using conversion factors mentioned in Eq.2, and this value was extrapolated to the hectare. Plot-wise NPP for the study period 2011-2014 are presented in **Table 8**. There was a significant ($F=14.16$, $p<0.002$) difference in NPP obtained across the plot for study period. Average annual NPP computed over the study period varied from 10.08±2.87 Mg ha^{-1} $year^{-1}$ to 5.65±1.45 Mg ha^{-1} $year^{-1}$. Plot-10 had the

highest mean NPP, while Plot-7 had the lowest NPP. Mixed forest species with large increment in their growth played a crucial role to attain highest NPP in Plot-10. Even though their total biomass was lower than the forest dominated by the single species like *Shorea robusta* (Plot-2, Plot-3, Plot-8 and Plot-9) their percent contribution in overall biomass increment was comparatively higher owing to their higher incremental growth rate (0.48cm $year^{-1}$) as well as all trees (100%) in the plot indicated increment in their growth across the study period. Whereas minimum NPP in Plot-7 was observed throughout the study period due to poor growth increment (0.21cm $year^{-1}$) as well as only 85% of trees in the plot showed increment in their growth, which was very low among all the plots. NPP values appeared to fluctuate across the plots from the year 2011 to 2014. Range of NPP was from 6.30±1.40 Mg ha^{-1} $year^{-1}$ (2014) to 10.07±2.51 Mg ha^{-1} $year^{-1}$ (2011) with an average of 8.20±2.14 Mg ha^{-1} $year^{-1}$.

Table 8: *Field based NPP of different sample plots in KNP for the period 2011-2014.*

		NPP (Mg ha^{-1} $year^{-1}$)				
Location	Plot	2011	2012	2013	2014	Mean±SD
Mukki	1	10.35	10.51	6.11	5.86	8.21±2.57
Supkhar	2	11.35	10.85	7.24	6.78	9.05±2.37
Supkhar	3	11.90	10.91	7.39	7.17	9.34±2.41
Bhaisanghat	4	12.00	10.35	6.22	7.32	8.97±2.67
Bhaisanghat	5	6.87	7.49	4.38	4.71	5.87±1.55
Kisli	6	12.95	9.27	8.05	5.68	8.99±3.03
Kisli	7	5.41	7.75	4.49	4.95	5.65±1.45
Kanha	8	8.60	8.87	5.11	4.37	6.74±2.33
Kanha	9	9.08	11.48	7.36	8.58	9.12±1.73
Sarhi	10	12.21	12.89	7.63	7.59	10.08±2.87

3.1.2 AMS tower data

Temperature-based radiation model: Incoming shortwave radiation is one of the crucial input parameters in CASA ecosystem model for simulating NPP of deciduous forest covers in KNP, BNP and MNP for the period 2011-2014. Owing to some technical issues, AMS towers in all the regions could record radiation until Dec. 2011, not up to Dec. 2014. Therefore, an air temperature based radiation model was developed in this study to obtain the radiation data for the subsequent study period. About 75% of the daily average (8AM-4PM) of half an hourly radiation data and corresponding air temperature data recorded across all the AMS tower locations between 2010 and 2011 was used to facilitate radiation modelling. Scatter plot between radiation and

temperature data obtained from AMS towers in KNP, BNP and MNP for the period 2010-2011 is depicted in **Figure 13a.**

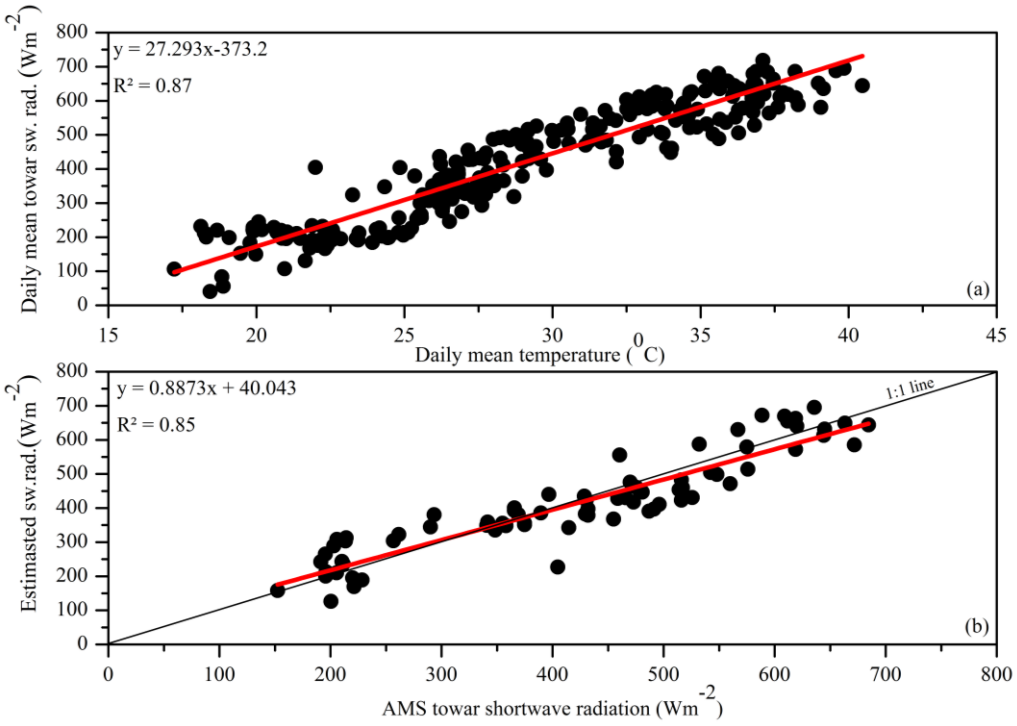

Figure 13: *Development and validation of radiation model.*

Significant correlation ($p < 0.05$) was observed between both the data sets with the coefficient of determination (R^2) 0.87, which implies that 87% of the radiation variability in all the regions can be linked to changes in air temperature, while the rest of the variance can be explained by other factors. Remaining 25% of the measured shortwave radiation was used for validation of the modelled radiation data. Scatter plot between 25% of the measured shortwave radiation by AMS tower and corresponding estimated radiation is presented in **Figure 13b**. There was a good agreement ($R^2 = 0.85$; $p < 0.05$) between both the data sets. The root-mean square error associated with estimated radiation was 58 Wm^{-2}, which was 14% of the mean tower radiation. Overall, mean radiation estimates by model (409 Wm^{-2}) was relatively lower than tower radiation (416 Wm^{-2}). Validation of the modelled radiation data indicates that the values coming from radiation model come close to the one year measured data satisfactorily over the study regions.

Variability of climate parameters: Based on daily temperature and rainfall values obtained from AMS tower, cumulated monthly rainfall, monthly average temperature and shortwave radiation (estimated from equation in **Figure 13**) were calculated and their characteristic seasonal pattern over KNP for the period 2011-2014 have been

depicted (**Figure 14**). These figures illustrate that rainfall seen mainly between June and September. Higher rainfall values appeared from July to September. More than 90% of the total rainfall in the season was received during this period. Maximum rainfall generally appeared in July, ranging from 371 mm (2011) to 548 mm (2013). Occasional winter rains occurred during December-February with the Northeast monsoon constituting 5% of the annual rainfall in the region. Maximum number of rainy days (99 days, i. e. days with rainfall of 2.5 mm or more) were found to be in 2013, while minimum rainy days was observed in 2012 (72 days). Annual rainfall over the study period varied from 1169 mm (2012) to 1642 mm (2013) with an average of 1331±215 mm. The region had received about 12% less rainfall in 2012 as compared to its mean annual rainfall. Seasonal temperature and radiation pattern over the region indicate that the pre-monsoon (March-May) season was very hot, with very high temperature and radiation values. Temperature during this period generally varied from 30^{o}C (March) to 37^{o}C (May). Consequently, radiation during the same period ranged from 438 Wm^{-2} to 654 Wm^{-2}. During September, there was a little rise in temperature and radiation values. Both the parameters fall rapidly from November which lasts until February. January was generally the coldest month with mean monthly temperature and radiation at 21 °C and 206 Wm^{-2}, respectively. Mean annual temperature ranged from 29.30 ^{o}C (2013) to 29.60 ^{o}C (2011) with an average of 29.40±0.13 ^{o}C. Mean annual solar radiation varied from 425 Wm^{-2} (2013) to 435 Wm^{-2} (2011) with an average radiation of 429±4 Wm^{-2}.

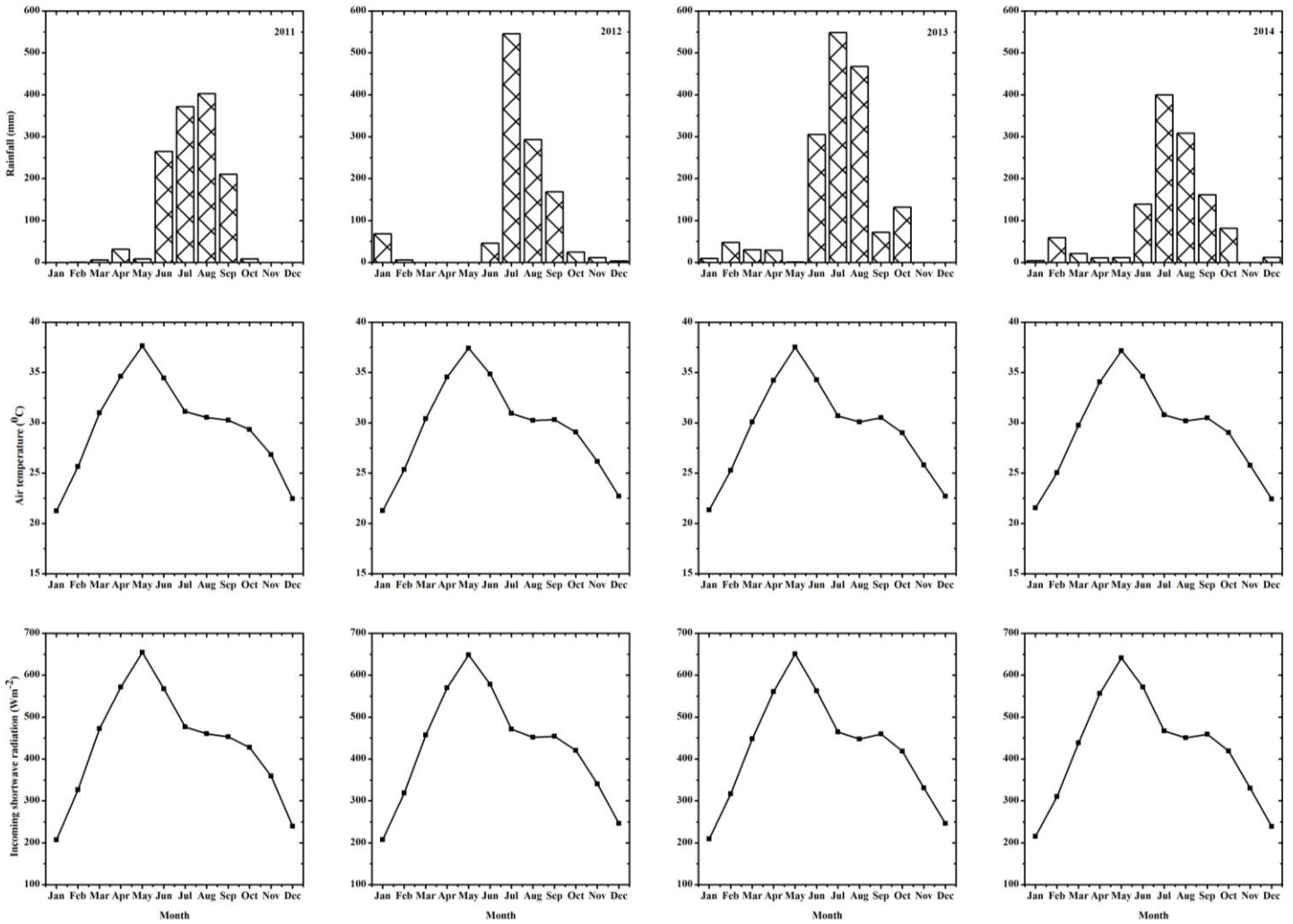

Figure 14: *Climate variability in KNP for the period 2011-2014.*

3.1.3 Satellite data analysis

Atmospheric correction: It was performed for all the satellite images using Fast Line-of-sight Atmospheric Analysis of Spectral Hyper cubes (FLAASH) atmospheric correction module. To undertake a detailed atmospheric correction, aerosol optical depth (AOD) covering the date of satellite pass over the study region was obtained from the MODIS (MOD08_M3, 0.55 µm) global AOD data product. Characteristic temporal profile of AOD over KNP varied from 0.18 – 0.62. It was found to be lower in winter months and higher in monsoon months. Initial visibility (km) was calculated from the AOD and it was appeared to be maximum in winter months (42.85 km) and minimum in monsoon months with 12.71 km. Top-of-Atmosphere (TOA) reflectance was computed for all the scenes to assess the influence of atmospheric constituents over the surface reflectance using the approach as outlined by (Pandya et al. 2007). Gain, offset and solar zenith angle information was obtained for all the scenes from their respective header files. Band specific E_0 (Exo-atmospheric solar irradiance) values were obtained from the literature (Landsat user guide). **Figure 15a-b** depicts 11 October 2010 Landsat false colour composite before (TOA, uncorrected) and after atmospheric correction (corrected) over the study region. The improvement in contrast between various features with edges between features could be seen in the corrected image. **Figure 15c-d** shows the histograms of TOA reflectance and atmospherically corrected reflectance for Red and NIR bands. Reduction in reflectance values and histograms shifting towards the origin were observed in red band after atmospheric correction. Correcting the atmospheric effects tends to decrease the reflectance values and introduces significant variations in the spectral reflectance in atmospherically corrected versus uncorrected spectral bands. The reflectance values in the NIR band increased after the atmospheric correction.

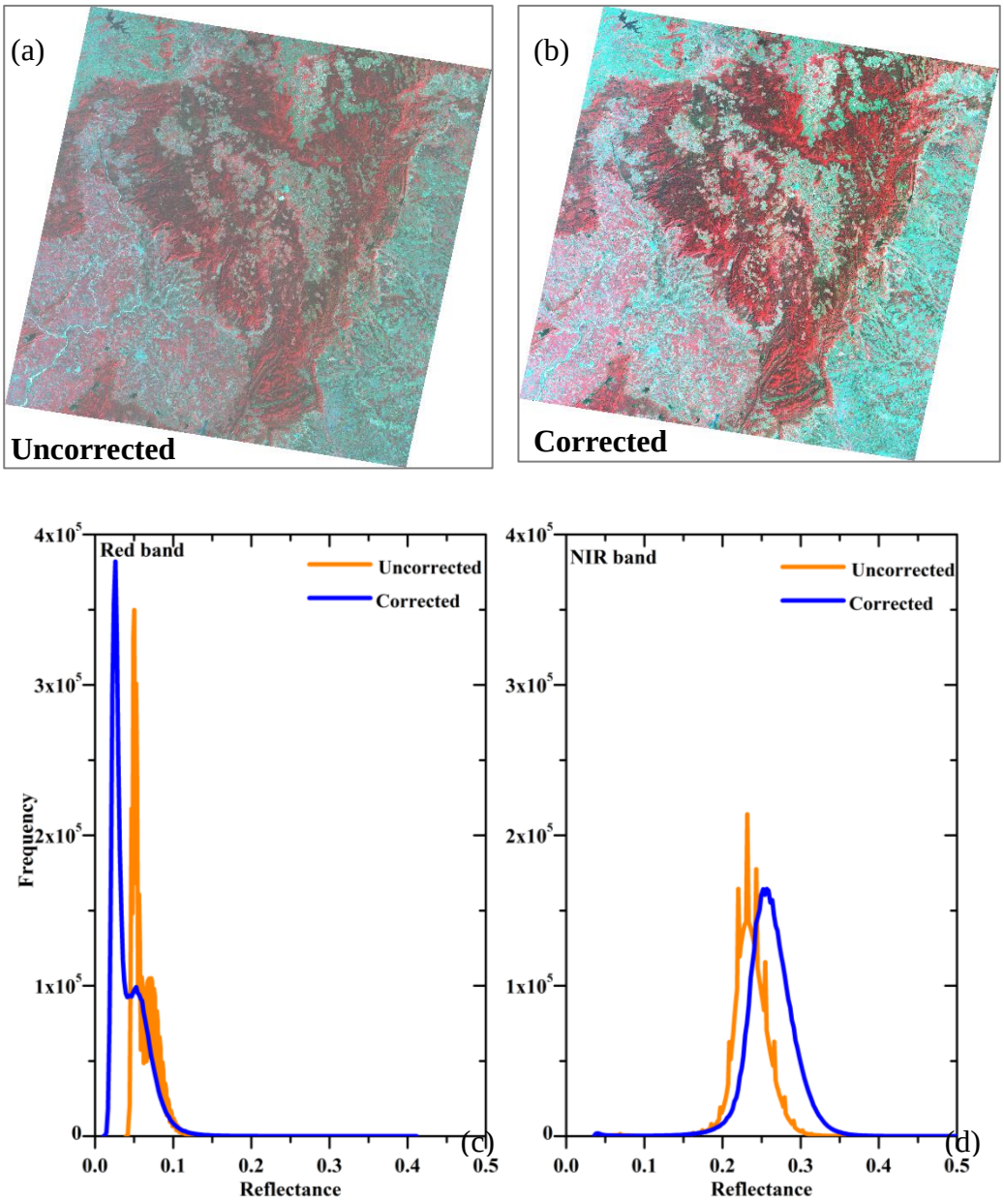

Figure 15: *Effect of atmospheric correction, a-b) uncorrected (TOA) and corrected Landsat scene, c-d) histograms of red and NIR band before and after atmospheric correction.*

KNP-LULC: Pure Landsat based multi-temporal images representing the three key phenological stages (start of senescence, leafless phase and full growth phase) of different deciduous forest types in KNP were used to generate landuse/landcover (LULC) map of the region. Multi-date satellite images acquired over KNP are depicted in **Figure 16**. Unsupervised classification scheme with more than 80 clusters were taken for image classification, of which eight LULC classes have been identified in the region.

Figure 16: *Multi-date Landsat satellite images coinciding with key phenological phases of deciduous forest in KNP.*

LULC map of KNP is shown in **Figure 17Figure 17:** Forest cover map of Kanha National Park. and statistics of the region generated from the classified output image is presented in **Table 9**. The table shows the spatial extent of land cover in square kilometres (km^2) and in percentages. Total geographical area of KNP estimated from satellite data was about 947 km^2. Forest classes with the largest area were Sal forest, mixed forest and Sal with bamboo forest. Although being similar, all the three forest types can be seen throughout the study area. Among them Sal forest constitutes bulk of the total geographical area of the park.

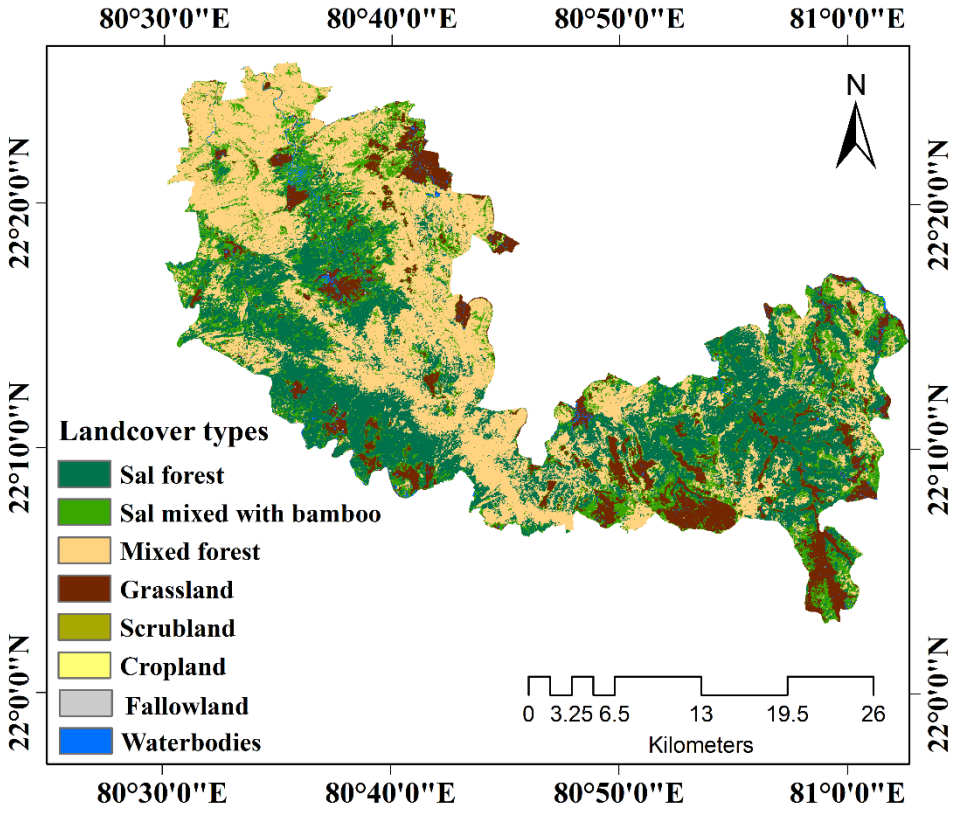

Figure 17: *Forest cover map of Kanha National Park.*

A quite large area of Sal forest can be seen in the Eastern (Supkhar and Bhaisanghat) and Southwestern (Mukki, Sondhar and Kisli) parts of the region. Part of Khatia, Ronda

and Kanha were also predominately covered with sal forest. Around 30.2% of the total area belongs to Sal forest with 286 km^2. Mixed forest covers most of the Northwestern (Sarhi and Kariwah) part of the region. The forest type covered with an area of 220 km^2 which is 23.2% of the total geographical area of the region. Sal with bamboo appeared throughout the study area that mostly surrounded by Sal forest. The forest type covered about 175 km^2 (18.5%) area of the park. Grassland and croplands can be recognised as scattered patches near the villages, covering about 155 km^2 (16.4%) of the area. Scrubland, fallow land and water bodies covered the remaining portion of the park.

Table 9: *Distribution of forest types in Kanha National Park.*

Class Code	Forest class	Area (Sq. km)	Percent of total area
1	Sal forest	286	30.2
2	Sal with bamboo	175	18.5
3	Mixed forest	220	23.2
4	Grassland	105	11.1
5	Scrubland	73	7.7
6	Cropland	50.0	5.3
7	Fallow land	23.0	2.4
8	Waterbodies	15.0	1.6
	Total	**947**	**100**

Accuracy assessment of LULC: This analysis was performed by comparing two sources of information one being the remote sensing based classified output images and other being the ground survey data (reference data). The reference data include information gathered at biomass sample plots as well as ground control points collected during field survey conducted for validating this LULC map. An analysis of comparison between these two data sets results in an error matrix, which was used to determine the overall accuracy of the classification. **Table 10** presented below illustrates the forest type wise Producer's and User accuracy achieved in the present study. Results shows that most of the classes possess producer accuracy higher than 85%; fallow land and water bodies gave the highest (100%) and cropland the lowest accuracy (66.7%). Except cropland, all the classes show a user accuracy between 81% and 100%, while the worst accuracy was possessed by the cropland (66.7%). A measure of overall behaviour of the unsupervised (ISODATA) classification can be determined by the overall accuracy, which was the total percentage of pixels correctly classified. The unsupervised classification yielded an overall accuracy of 90% in KNP, indicating very high agreement with the ground truth.

Table 10: *Classification accuracy assessment report for KNP.*

Class code	Class name	Reference Totals	Classified Totals	Number Correct	Producers Accuracy (%)	Users Accuracy (%)
1	Sal forest	28	27	26	92.9	96.3
2	Sal with bamboo	14	12	12	85.7	100.0
3	Mixed forest	26	26	24	92.3	92.3
4	Grassland	10	10	9	90.0	90.0
5	Scrubland	10	11	9	90.0	81.8
6	Cropland	6	6	4	66.7	66.7
7	Fallow land	4	4	4	100.0	100.0
8	Waterbodies	6	6	6	100.0	100.0
	Total	**104**	**102**	**94**		

Overall accuracy=90%

CASA NPP modelling: Spatial and temporal variability of deciduous forest NPP in KNP was estimated using CASA ecosystem model based on multi-temporal Landsat images and meteorological data recorded at AMS stations. The model simulates NPP in terms of carbon stock (MgC ha^{-1} $year^{-1}$), whereas field measured NPP obtained in this study were in biomass stock (Mg ha^{-1} $year^{-1}$). However to make CASA NPP comparable with the field measured NPP, all the CASA simulated NPP values were converted to biomass stock by assuming that the biomass stock was 2.08 times of the carbon sequestered by terrestrial vegetation (Brown and Lugo, 1982; Ravindranath et al., 1997). CASA simulated NPP presented hereafter are in biomass stock (Mg ha^{-1} $year^{-1}$). **Figure 18**: Spatial variability of NPP over KNP for the period 2011-2014. depicts CASA simulated NPP over KNP from 2011 to 2014. The Eastern part of the region was occupied by huge Sal trees, where conditions were favourable for vegetation growth due to the presence of perennial and seasonal water bodies. On the otherhand, parts of Western region (Ronda, Kanha, etc) consists of mixed forest type with poor tree density. Therefore, NPP in the Western part was generally lower than that of the area in the East part of KNP, which can be seen in **Figure 18**: Spatial variability of NPP over KNP for the period 2011-2014. Using the landcover information (**Figure 17**), Sal forest, Sal forest mixed with bamboo were distinguished as predominant landcover types in the Eastern parts of the region. While mixed forest was the major landcover in Western part of the region. Average NPP of the four years of these forest types varied significantly as value of Sal forest (8.94 Mg ha^{-1} $year^{-1}$) > Sal mixed with bamboo (8.32 Mg ha^{-1} $year^{-1}$) > mixed forest (7.48 Mg ha^{-}

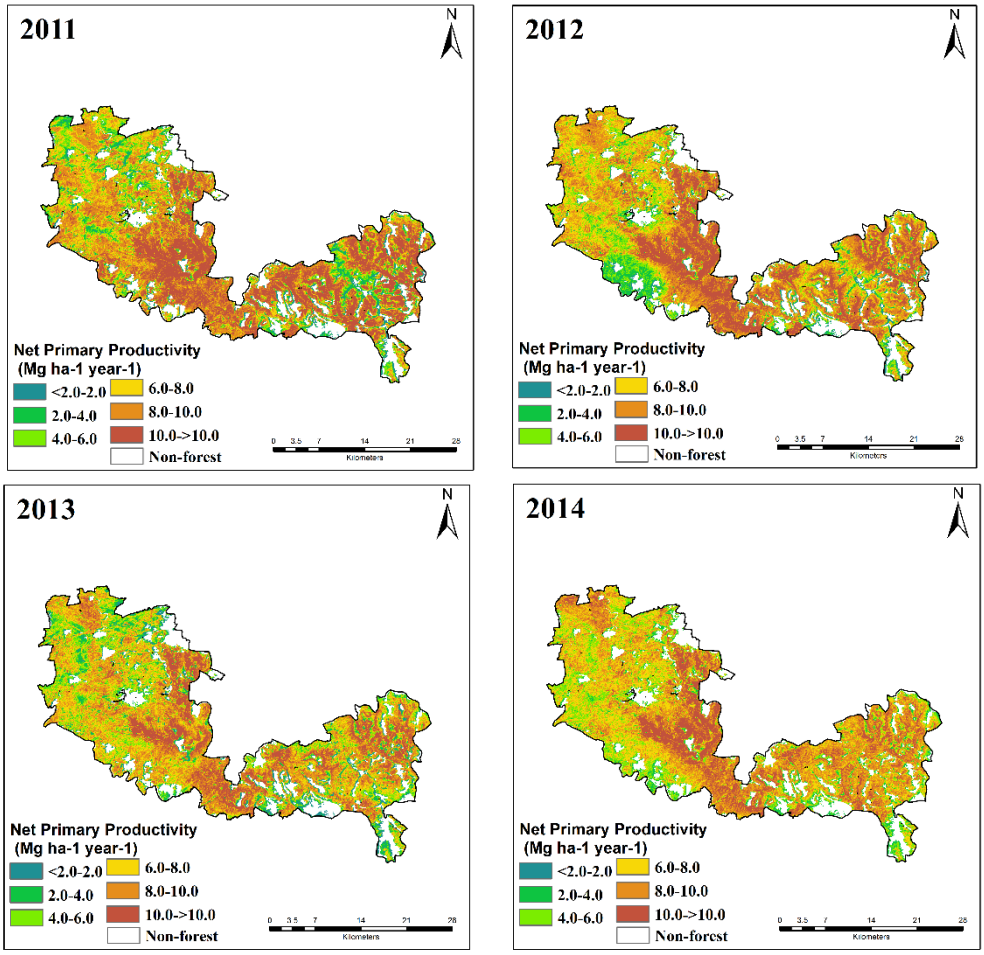

***Figure 18**: Spatial variability of NPP over KNP for the period 2011-2014.*

^{1} year^{-1}). NPP was found to be higher in the forests of Eastern region due to favourable microclimate conditions induced by the topographic variations. NPP was appeared to be minimum in the Western parts of the region due to poor tree density and growth which is in turn due to lack of water sources. In order to understand the temporal variation of NPP over the study period, NPP values of three predominant vegetation types with the temporal change was made. It indicates that the NPP values varied little with the temporal change except that the NPP of all vegetation types was relatively lower in 2013 as compared to other years. CASA simulated NPP obtained for different sample plots in KNP for the period 2011-2014 is presented in **Table 11**. Wide variation in simulated NPP (4.47 Mg ha^{-1} year^{-1} to 12.8 Mg ha^{-1} year^{-1}) values across the plots was because of marked variations in species composition, tree density, canopy spread etc. High value of NPP was found concentrated in Plot-10 (NPP averaged across the study period, 10.06±2.64 Mg ha^{-1} year^{-1}) followed by Plot-3 (9.52±.38 Mg ha^{-1} year^{-1}) which was mainly attributed to the large tree density and significant tree growth in both the plots. Whereas, the

lowest NPP was associated with Plot-7 (6.44±1.53 Mg ha^{-1} $year^{-1}$) followed by Plot-5 (6.48±1.41 Mg ha^{-1} $year^{-1}$) due to existence of mixed forest type with poor growth. NPP averaged across the plots was found to be highest in 2012 (9.88±2.3 Mg ha^{-1} $year^{-1}$), followed by 2011 (9.73±2.28 Mg ha^{-1} $year^{-1}$), while the lowest NPP (6.71±1.22 Mg ha^{-1} $year^{-1}$) was appeared in 2014.

Table 11: *CASA simulated deciduous forest NPP for different sample plots in KNP for the period 2011-2014.*

		NPP (Mg ha^{-1} $year^{-1}$)				
Location	Plot	2011	2012	2013	2014	Mean±SD
Mukki	1	9.61	10.13	6.55	6.49	8.2±1.95
Supkhar	2	10.63	12.15	6.55	7.36	9.17±2.65
Supkhar	3	11.42	10.05	9.15	7.49	9.53±1.65
Bhaisanghat	4	11.48	8.15	6.61	7.32	8.39±2.15
Bhaisanghat	5	6.93	7.95	4.56	6.49	6.48±1.42
Kisli	6	12.29	9.30	9.15	5.93	9.17±2.6
Kisli	7	5.16	8.57	6.64	5.45	6.45±1.55
Kanha	8	8.59	9.26	6.55	4.47	7.22±2.16
Kanha	9	9.40	10.36	8.65	8.67	9.27±0.8
Sarhi	10	11.84	12.79	8.01	7.59	10.06±2.64

CASA NPP validation: Deciduous forest NPP simulated from the CASA ecosystem model was validated using field measured NPP obtained for different sample plots (**Table 8**) in KNP for the period 2011-2014. Scatter plot between CASA NPP and field based NPP is depicted in **Figure 19**. There was a good agreement between both the data sets with coefficient of determination (R^2) 0.93, explaining 93% variability at 95% confidence level. The mean values of ground and simulated NPP are 8.19 Mg ha^{-1} $year^{-1}$ and 8.40 Mg ha^{-1} $year^{-1}$, respectively. Mean NPP estimated by the CASA model was relatively higher than the field measured NPP with the root-mean square error of 0.76 Mg ha^{-1} $year^{-1}$, which is 9.43% of the mean observed NPP over the region.

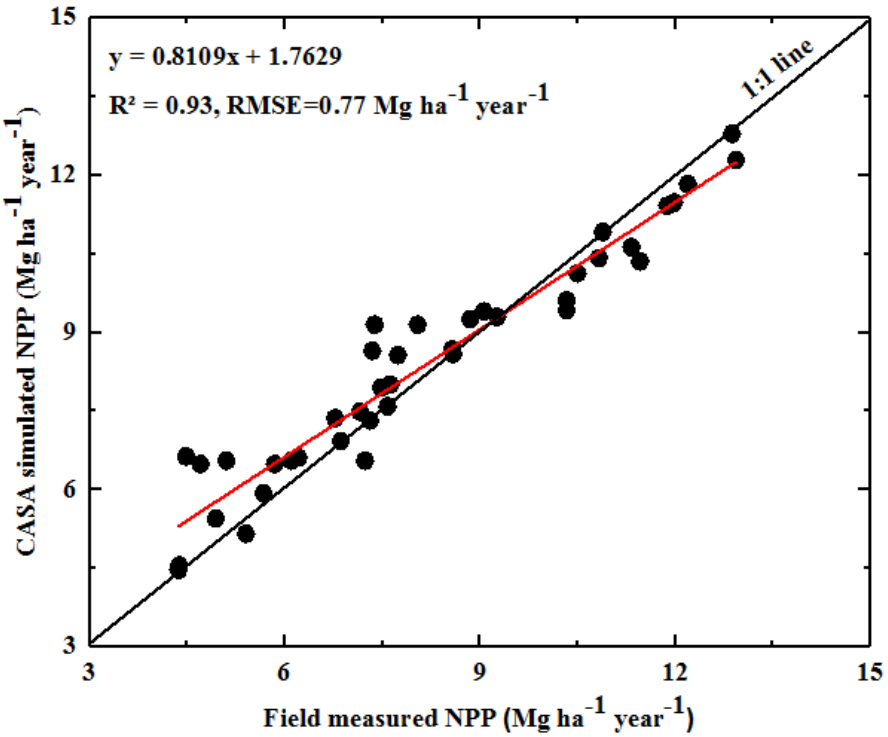

Figure 19: *Scatter plot describing the correlation between fields measured NPP and CASA derived NPP over KNP for the period 2011-2014.*

3.2 Bandhavgadh National Park

3.2.1 Field inventory: In the 10 quadrates of 0.1 ha laid down at BNP, there were 466 trees whose DBH was ≥ 3.18 cm and represented by 45 tree species. Plot-wise distribution of tree types with their percentage contribution to the total tree population is presented in **Appendix 8**. Of the 45 species, eight species indicated stand density of >2%, whereas 37 species showed stand density ≤ 2% of the total tree population. Out of all the tree species Sal tree was found to be maximum with the presence of 96 trees, which was estimated to be 20.6% of the measured tree density (466 trees) followed by *Lagerstroemia parviflora* (Lendia) with 12%. Descriptive statistics of the sample plots studied in BNP is presented in **Table 12**. Amongst all the sample plots, Plot-9 contained the greatest stand density of 101 trees, while Plot-5 witnessed the lowest tree density with 15 trees. Analysis of the variance in tree height revealed significant variations ($F=6.48$, $p<0.05$) between the sample plots from 25.13±3.33m in Plot-5 to 7.48 ±0.76m in Plot-2. DBH of the stand varied across the plots ($F=27.83$, $p<0.05$). It was found to be very high in plot-5 (46.95±11.67cm) followed by Plot-11 (30.45±16.31cm), whereas poor DBH was observed in Plot-9 (9.0±9.58cm).

Table 12: *Descriptive statistics of different sample plots in BNP.*

Location	Plot	Tree density/ 0.1 ha	Average tree height (m) ±SD	Average DBH (cm)±SD
Tala	1	35	7.52±2.29	14.49±7.14
Tala	2	31	7.48±0.76	17.92±9.22
Tala	3	34	11.52±6.31	22.47±18.61
Tala	4	36	13.93±7.81	20.78±12.54
Tala	5	15	25.13±3.33	46.95±11.67
Pataur	6	58	9.92±4.93	12.93±5.87
Pataur	7	27	15.20±7.33	17.33±11.97
Kallwah	8	81	8.76±5.69	10.77±9.78
Kallwah	9	101	9.66±4.74	9.0±9.58
Magdhi	10	48	12.68±5.69	20.79±11.20

Aboveground biomass (AGB): AGB estimation was carried out for each trees species of different classes in each sample plot for the period 2010-2014. Per plot biomass (0.1ha) was determined by summing up the biomass of different individuals occurring in the each plot. After calculating per plot AGB (kg/0.1ha), the total biomass was calculated in megagrams per hectare (Mg ha^{-1}), and these values were extrapolated to the hectare using Eq.2. Plot-wise biomass per hectare for the period 2010-2014 is

presented in **Table 13**. AGB varied considerably across the plots from 61 Mg ha^{-1} to 380 Mg ha^{-1}. It was found to be maximum across the study period in Plot-5 with an average of 371.89±7.9 Mg ha^{-1}, ranging from 362 Mg ha^{-1} (2010) to 381Mg ha^{-1} (2014). Least biomass storage was accounted across the study period in Plot-1 with an average biomass of 76.17±10.7 Mg ha^{-1}, varied from 61.2 Mg ha^{-1} (2010) to 84.4 Mg ha^{-1} (2014). AGB averaged across the plots was found to be highest in 2014 (196.7±99 Mg ha^{-1}), whereas the lowest AGB (174±99 Mg ha^{-1}) was observed in 2010.

Table 13: *AGB for different sample plots in BNP for the period 2010-2014.*

		AGB (Mg ha^{-1})					
Location	Plot	2010	2011	2012	2013	2014	Mean±SD
Tala	1	61.23	68.46	83.76	82.92	84.47	76.17±10.7
Tala	2	95.84	99.96	113.41	109.90	114.45	106.71±8.4
Tala	3	256.41	262.07	284.09	276.51	286.80	273.17±13.4
Tala	4	273.40	277.55	289.49	282.48	292.24	283.03±7.9
Tala	5	361.93	366.07	377.98	372.56	380.91	371.89±7.9
Pataur	6	80.69	86.63	101.99	94.10	103.72	93.43±9.9
Pataur	7	102.55	108.03	122.75	120.37	125.03	115.75±9.9
Kallwah	8	141.77	146.80	164.25	163.90	166.08	156.56±11.4
Kallwah	9	147.17	153.60	167.38	166.08	171.60	161.17±10.3
Magdhi	10	219.33	223.67	239.99	238.75	242.20	232.79±10.5

Plot-wise inter-annual variation in different tree attributes are presented in **Appendix 9**. Of the 10 plots studied in BNP, 99% of trees in Plot-1, while only 71% of the trees in Plot-3 indicated increment in their growth (DBH), which were the highest and lowest among all the plots. About 74%-86% of trees in the remaining plots were exhibited increment in their DBH. About 91% of trees across the plots showed increment in 2014, whereas only 64% of trees indicated increment in 2011. Rate of increment in DBH was another crucial biophysical parameter, where large variation in AGB was observed due to variation in DBH across the plots. Increment in DBH was comparatively higher in mixed forest rather than in forest dominated by single species. Plots those covered with mixed forest species indicated an average increment in the range of 0.85cm year^{-1} (Plot-1) to 0.44cm year^{-1} (Plot-2 and Plot-3). Whereas plots which were dominated by single species showed increment between 0.25cm year^{-1} (Plot-2) and 0.36cm year^{-1} (Plot-8). Plot-4 showed the lowest increment among all the plots with 0.27cm year^{-1}. Though only 81% of trees across the plots showed increment in 2012, but mean increment in DBH was found to be highest in 2012 with 0.63cm year^{-1}, while the lowest increment was observed in 2014 with an average of 0.36cm year^{-1}. Relative deviation (RD%) in

AGB across the study years is presented in **Appendix 10**. RD in AGB represented as $RD(\%)=100*((AGB_i-AGB_{2010})/AGB_{2010})$, where i represent AGB in 2011, 2012, 2013 and 2014, respectively. RD across the plot was found to be highest in 2014 with an average of 17.6%. Whereas the lowest change in AGB was observed in 2011 with a mean of 4.36%. Mean change in AGB across the study period was maximum at Plot-1 (30.5%), whereas minimum change in AGB was observed in Plot-5 (3.4%).

Field based NPP : Net primary productivity (NPP) of the tree species lying within the sample plots was estimated by dividing change in their AGB (ΔAGB) with time difference (Δt). More specifically, ΔAGB is the difference between current AGB (t2) and the back calculated AGB (t1). NPP value thus obtained was kg/0.1ha/year. After calculating NPP per plot, total NPP was calculated in megagrams per hectare per year (Mg ha^{-1} $year^{-1}$) using conversion factors given in Eq.2, and this value was extrapolated to the hectare. Plot wise NPP estimated for the study period are presented in **Table 14**. Average annual NPP computed over the study period varied from 8.45±3.68 Mg ha^{-1} $year^{-1}$ to 5.11±2.0 Mg ha^{-1} $year^{-1}$. Plot-3 had the highest mean NPP, while Plot-5 holds the lowest NPP.

Table 14: *Field based NPP for different sample plots in BNP for the period 2011-2014.*

		NPP (Mg ha^{-1} $year^{-1}$)				
Location	Plot	2011	2012	2013	2014	Mean±SD
Tala	1	7.23	11.26	7.23	5.81	7.88±2.35
Tala	2	4.12	8.79	4.69	4.65	5.56±2.16
Tala	3	5.66	13.84	6.70	7.60	8.45±3.68
Tala	4	4.15	8.05	3.03	4.71	4.98±2.16
Tala	5	4.14	8.03	3.54	4.75	5.11±2.0
Pataur	6	5.94	10.65	4.47	5.76	6.7±2.71
Pataur	7	5.48	10.10	5.94	5.62	6.79±2.22
Kallwah	8	5.03	11.24	7.38	6.08	7.43±2.72
Kallwah	9	6.43	10.11	6.30	6.11	7.24±1.92
Magdhi	10	4.34	10.33	6.47	5.72	6.71±2.57

Even though AGB stock of mixed forest plot (Plot-3) was comparatively lower than the forest dominated by single species like *Shorea robusta* (Plot-5) but their percent contribution in overall biomass increment was comparatively higher than forest dominated by single species. Whereas minimum NPP was observed throughout the study period in Plot-5 due to poor increment in DBH (0.32cm $year^{-1}$) as well as only 78% of trees in the plot showed increment in their growth. NPP values appeared to

fluctuate across the plots from 2011 to 2014. Range of NPP was from 5.25±1.1 Mg ha^{-1} $year^{-1}$ (2011) to 10.24±1.73 Mg ha^{-1} $year^{-1}$ (2012) with an average of 6.69±2.38 Mg ha^{-1} $year^{-1}$.

3.2.3 Variability of climate parameters

Based on daily temperature and rainfall values obtained from AMS tower, cumulated monthly rainfall, average monthly temperature and average monthly shortwave radiation (estimated from equation in **Figure 13**) were calculated and their characteristic seasonal pattern over BNP for the period 2011-2014 have been depicted in **Figure 20:** Climate variability in BNP during the study period.. These figures illustrate that rainfall seen mainly between June and September. Higher rainfall values appeared from July to September. More than 88% of the total rainfall in the season was received during this period. Maximum rainfall was generally appeared in August, ranging from 180 mm (2014) to 416 mm (2013). Occasional winter rains were occurred during December-February with the Northeast monsoon constituting 5% of the annual rainfall in the region. Maximum number of rainy days (82 days, i. e. days with rainfall of 2.5 mm or more) were found to be in 2013, while minimum rainy days were observed in 2014 (62 days). Annual rainfall of the region varied across the study period from 923 mm (2014) to 1322 mm (2013) with an average of 1118±171 mm. The region had received about 18% less rainfall in 2014 as compared to its mean annual rainfall. Seasonal temperature and radiation pattern over the region indicate that the pre-monsoon (March-May) season was very hot, with very high temperature and radiation values. Temperature during this period generally varied from 26 ^{o}C (March) to 37 ^{o}C (May). Consequently, radiation during the same period ranged from 360 Wm^{-2} to 640 Wm^{-2}. During September, there was a little rise in temperature and radiation values. Both the parameters fall rapidly from November which lasts until February. January was generally the coldest month with mean monthly temperature and radiation at 19 °C and 158 Wm^{-2}, respectively. Mean annual temperature ranged from 28.27 ^{o}C (2013) to 28.57 ^{o}C (2012) with an average of 28.43±0.11 ^{o}C. Mean annual solar radiation varied from 398 Wm^{-2} (2013) to 406 Wm^{-2} (2012) with an average radiation of 403±137 Wm^{-2}.

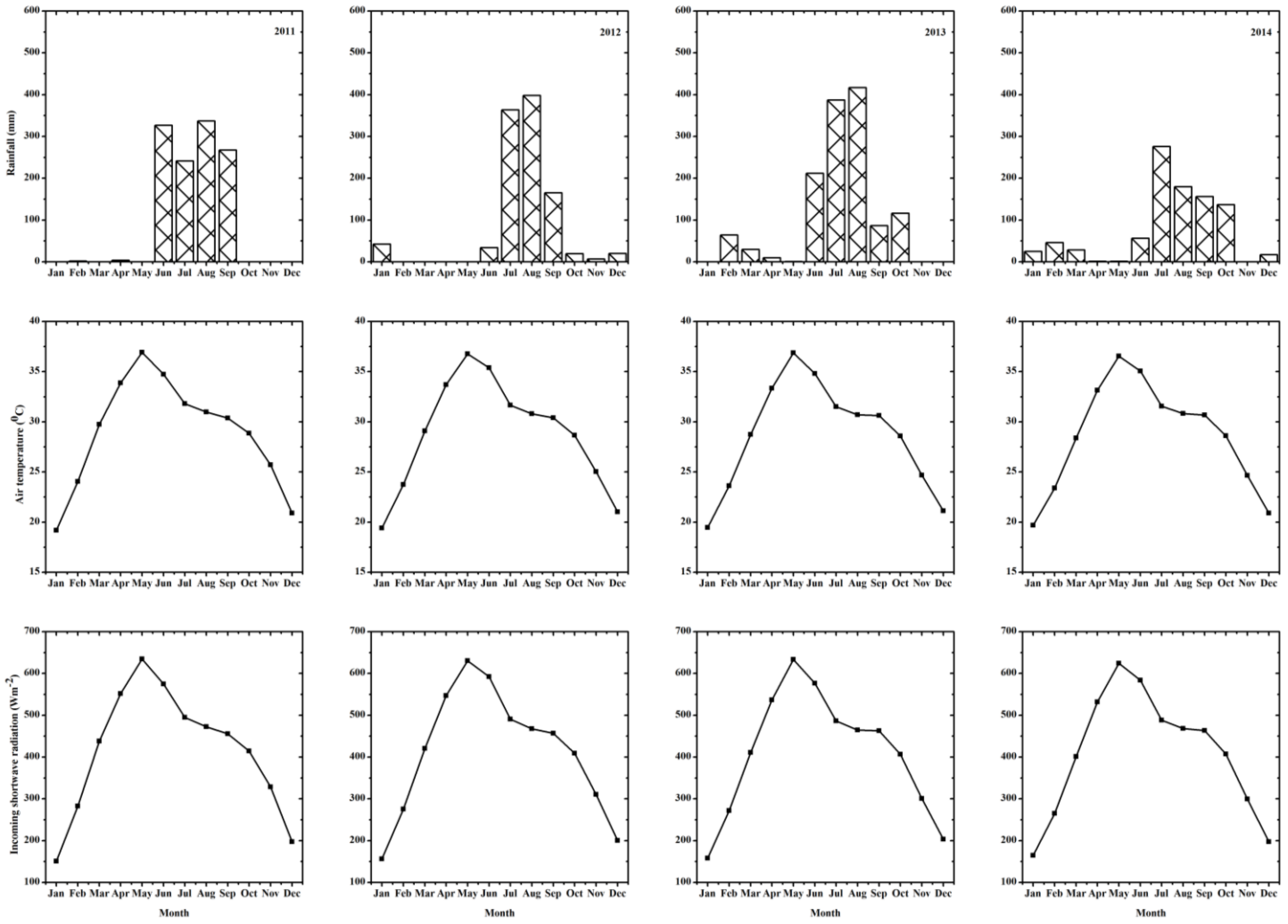

Figure 20: *Climate variability in BNP during the study period.*

3.2.3 Satellite data analysis

Atmospheric correction: It was performed for all the satellite images using Fast Line-of-sight Atmospheric Analysis of Spectral Hyper cubes (FLAASH) atmospheric correction module. To undertake a detailed atmospheric correction, aerosol optical depth (AOD) covering the date of satellite pass over the study region was obtained from the MODIS (MOD08_M3, 0.55 µm) global AOD data product. Characteristic temporal profile of AOD over BNP varied from 0.15 – 0.58. It was found to be lower in winter months and higher in monsoon months. Initial visibility (km) calculated from the AOD appeared to be maximum in winter months (52.1 km) and minimum in monsoon months with 13.41 km. **Figure 21a-b** depicts 23 October 2010 Landsat false colour composite before (TOA, uncorrected) and after atmospheric correction (corrected) over the study region. The improvement in contrast between various features with edges between features could be seen in the corrected image. **Figure 21c-d** shows the histograms of TOA reflectance and atmospherically corrected reflectance for Red and NIR bands of Landsat satellite data. Reduction in reflectance values and histograms shifting towards the origin were observed in red band after atmospheric correction, whereas the reflectance values in the NIR band increased after the atmospheric correction.

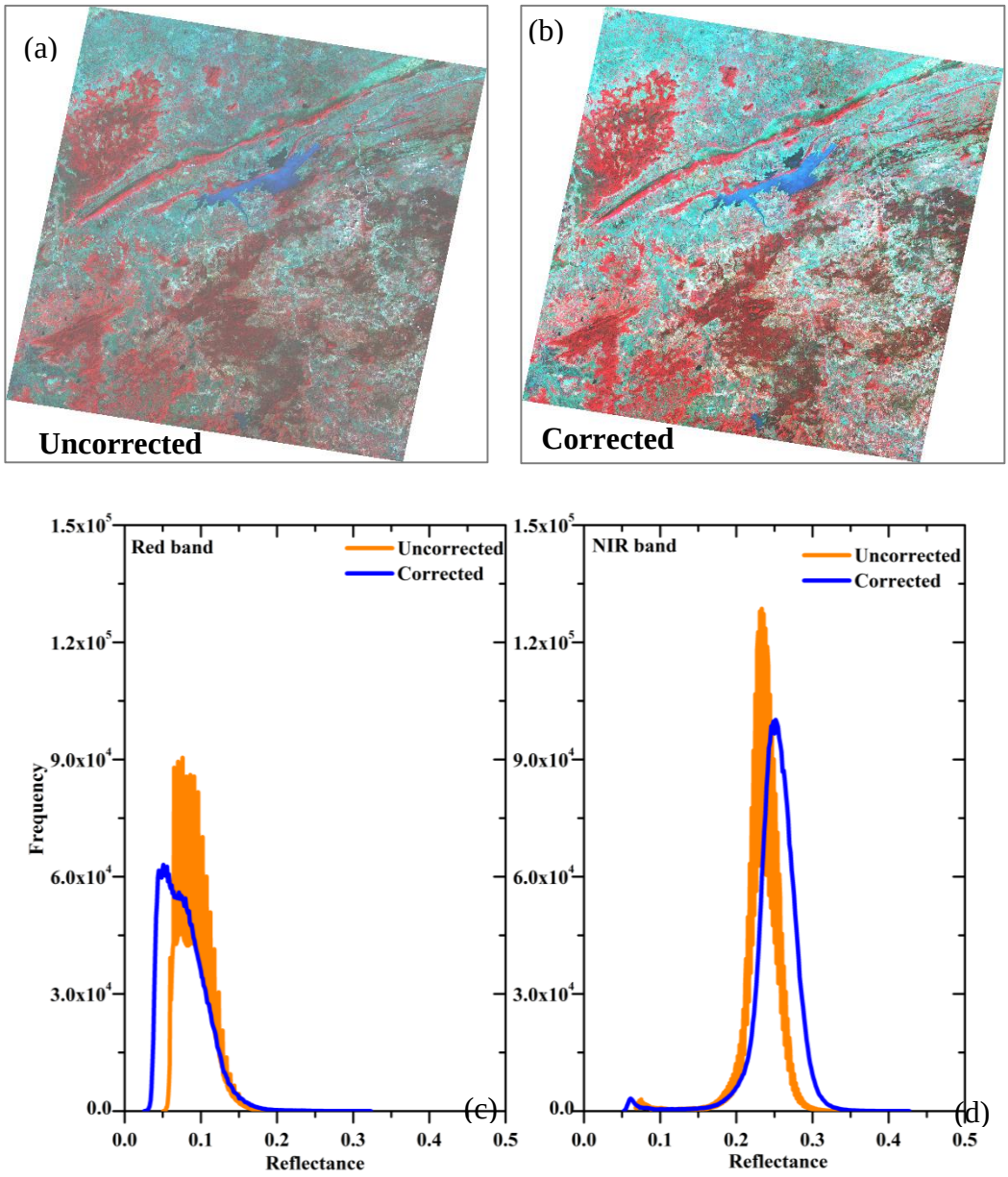

Figure 21: *Effect of atmospheric correction, a-b) uncorrected (TOA) and corrected Landsat scene, c-d) histograms of red and NIR band before and after atmospheric correction.*

BNP-LULC: Landsat based multi-temporal images representing three key phenological stages (start of senescence, leafless phase and full growth phase) of different deciduous forests in BNP were used to generate anduse/landcover (LULC) map of the region. Multi-date satellite images acquired over the region are depicted in **Figure 22**. Unsupervised classification scheme with more than 80 clusters were taken for image classification, of which eight LULC classes have been identified in the region.

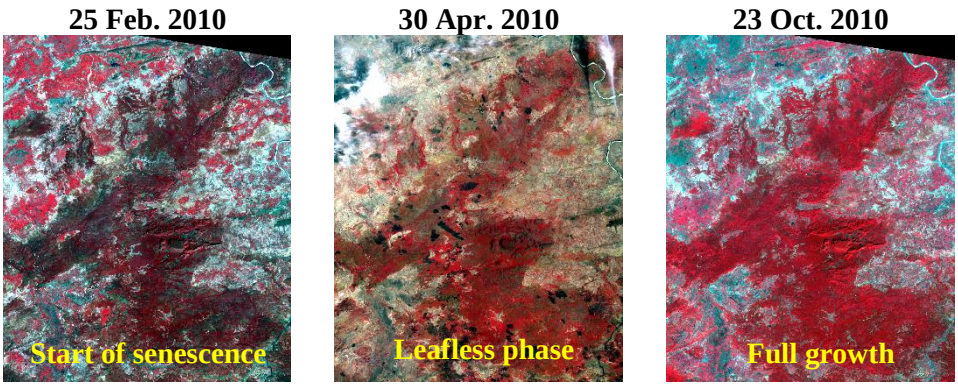

Figure 22: *Multi-date Landsat 5 TM satellite images coinciding with key phenological phases of deciduous forests in BNP.*

LULC of BNP is shown in **Figure 23** and statistics of the region generated from the classified output image is presented in **Table 15**. The table shows the spatial extent of land cover in square kilometre (km^2) and in percentages. Total geographical area of BNP estimated from satellite data was about 697.3 km^2. Mixed forest dominated by Sal (Sal mixed forest) constitutes bulk of the total geographical area of the park. Around 42.16% of the total area belongs to the mixed forest dominated by Sal with 294 km^2. Mixed forest was the second largest forest cover in the region with 180 km^2 (25.81%) followed by mixed forest dominated by Lendia with an area about 170 km^2 (24.38%). Grassland, Scrubland, Fallow land and Water bodies form the remaining portion of the park.

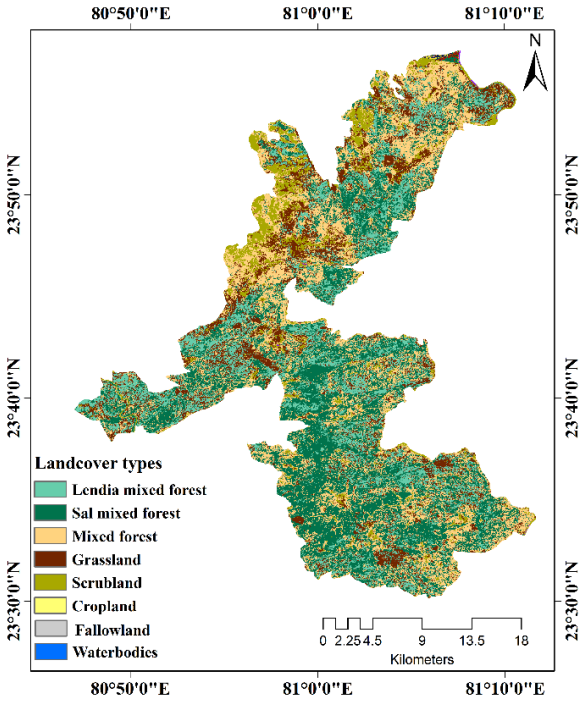

Figure 23: *Forest cover map of Bandhavgadh National Park.*

Table 15: *Distribution of forest types in Bandhavgadh National Park.*

Class code	Forest class	Area (Sq. km)	Percent of total area
1	Mixed forest dominated by Lendia	170	24.38
2	Mixed forest dominated by Sal (Sal mixed forest)	294	42.16
3	Mixed forest	180	25.81
4	Grassland	5.4	0.77
5	Scrubland	15	2.15
6	Cropland	14.3	2.05
7	Fallow land	3.6	0.52
8	Waterbodies	170	2.15
	Total	**697.3**	**100**

Accuracy Assessment of the classified image: This analysis was performed by comparing two sources of information one being the remote sensing based classified output image and other being the ground survey data (reference data). The reference data include information gathered at biomass sample plots as well as ground control points collected during field survey especially conducted for validating this LULC map. The relationship between these two data sets results an error matrix, which was used to determine the overall accuracy of the classification. Forest type wise Producer's and User accuracy achieved in the present study are presented in **Table 16**.

Table 16: *Classification accuracy assessment report of BNP.*

Class code	Class name	Reference Totals	Classified Totals	Number Correct	Producers Accuracy (%)	Users Accuracy (%)
1	Mixed forest dominated by Lendia	15.0	18.0	15.0	100.0	83.3
2	Mixed forest dominated by Sal	21.0	20.0	18.0	85.7	90.0
3	Mixed forest	15.0	16.0	15.0	100.0	93.8
4	Grassland	12.0	12.0	9.0	80.0	100.0
5	Cropland	5.0	4.0	3.0	60.0	75.0
6	Scrubland	4.0	3.0	3.0	75.0	100.0
7	Fallow land	5.0	4.0	4.0	80.0	100.0
8	Waterbodies	2.0	2.0	2.0	100.0	100.0
	Total	**79**	**79**	**70**		

Overall accuracy=87%

Results indicated that producer's accuracy varied between 60% and 100%. Mixed forest and mixed forest dominated by Lendia forest possess the highest accuracy with 100%,

whereas cropland showed the poor accuracy with 60%. Except cropland, all the classes show a user accuracy between 90% and 100%, while the worst accuracy was possessed by the cropland (60%). A measure of overall behaviour of the unsupervised (ISODATA) classification can be determined by the overall accuracy, which was the total percentage of pixels correctly classified. The unsupervised classification yielded an overall accuracy of 87% in BNP, indicating very high agreement with the ground truth information.

CASA NPP modelling: Spatial and temporal variability of deciduous forest NPP in BNP was estimated using CASA ecosystem model based on multi-temporal Landsat images and meteorological data recorded at AMS towers for the period 2011-2014. CASA model simulates NPP in terms of carbon stock (MgC ha^{-1} $year^{-1}$), whereas field measured NPP obtained in this study were in biomass stock (Mg ha^{-1} $year^{-1}$). However, to make CASA NPP comparable with the field measured NPP, all the CASA NPP values were converted to biomass stock by assuming that the biomass stock was 2.08 times of the carbon sequestered by terrestrial vegetation (Sandra Brown and Lugo 1982; Ravindranath, Somashekhar, and Gadgil 1997). CASA simulated NPP presented hereafter are in biomass stock (Mg ha^{-1} $year^{-1}$). **Figure 24** depicts CASA simulated NPP over BNP from 2011 to 2014. Central part of the region is mainly occupied by Sal mixed forest in the valleys and on the lower slopes, where conditions are favourable for vegetation growth due to presence of several perennial and seasonal water bodies. While North West part of the region was largely covered by mixed forest, grassland and scrubland due to lack of water sources. Therefore, NPP of the North West part was generally lower than that of the area in Central part of BNP, which can be seen from **Figure 24**. Using the landcover information (**Figure 23**), mixed forest dominated by Sal, mixed forest dominated by Lendia and mixed forest were distinguished as predominant landcover types in the Central and Southern parts of the region. While mixed forest, grassland and scrubland were the major landcover types in the North part of the region. Average NPP of the four years of these forest types varied considerably as value of mixed forest dominated by Sal (9.36 Mg ha^{-1} $year^{-1}$) > mixed forest dominated by Lendia (7.9 Mg ha^{-1} $year^{-1}$) > mixed forest (7.0 Mg ha^{-1} $year^{-1}$). NPP was found to be higher in forests of the Central and South part of the region. NPP was appeared to be minimum in Northwestern parts of the region. In order to understand

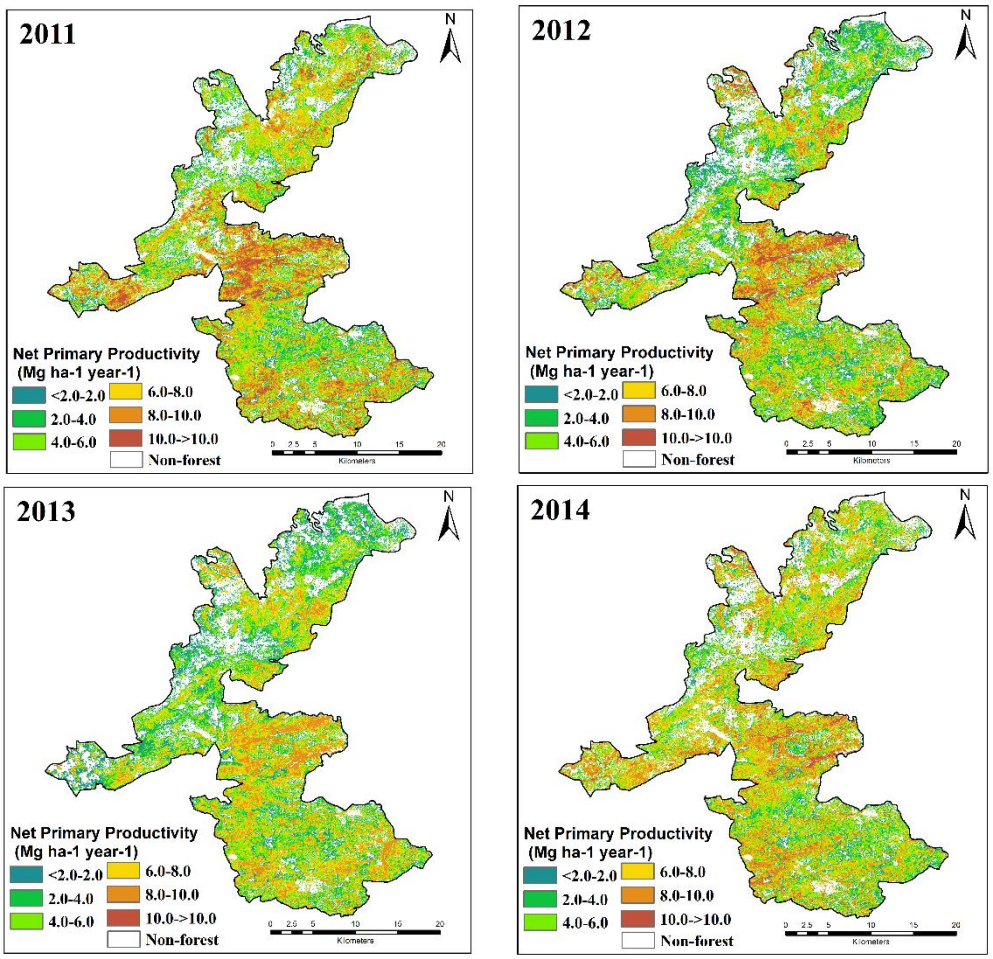

Figure 24: *Spatial variability of NPP over BNP for the period 2011-2014.*

temporal variation of NPP over the study period, NPP values of the predominant vegetation types with the temporal change was made. Results indicate that NPP values varied little with temporal change except that NPP of all vegetation types was lower in 2014 when compared to their NPP in other years. CASA simulated NPP for different sample plots in BNP for the period 2011-2014 is presented in **Table 17**. Wide variation in simulated NPP was observed between the plots from 4.47 Mg ha^{-1} $year^{-1}$ to 14.23 Mg ha^{-1} $year^{-1}$. High NPP was found concentrated in the Plot-3 (9.6±3.12 Mg ha^{-1} $year^{-1}$) followed by Plot-1 (8.71±2.35 Mg ha^{-1} $year^{-1}$). The lowest NPP (6.01±1.48 Mg ha^{-1} $year^{-1}$) was found be with Plot-5. NPP averaged across the plots was found to be highest in 2012 (10.55 Mg ha^{-1} $year^{-1}$), while the lowest NPP (5.98 Mg ha^{-1} $year^{-1}$) was appeared in 2011.

Table 17: *CASA simulated deciduous forest NPP for different sample plots in BNP for the period 2011-2014.*

		NPP (Mg ha^{-1} year^{-1})				
Location	Plot	2011	2012	2013	2014	Mean±SD
Tala	1	9.11	11.69	7.97	6.05	8.7±2.35
Tala	2	4.47	9.17	5.47	5.57	6.17±2.06
Tala	3	7.99	14.23	7.57	8.65	9.61±3.11
Tala	4	4.91	8.67	4.91	5.91	6.1±1.78
Tala	5	5.01	8.15	5.82	5.05	6.01±1.48
Pataur	6	5.70	11.15	5.26	6.61	7.18±2.7
Pataur	7	5.93	10.28	6.82	7.43	7.61±1.88
Kallwah	8	5.22	11.84	7.68	5.08	7.45±3.16
Kallwah	9	6.57	10.67	7.80	6.18	7.81±2.03
Magdhi	10	4.89	9.61	7.76	7.65	7.48±1.95

CASA-NPP validation: Deciduous forest NPP simulated from the CASA ecosystem model was validated using field measured NPP obtained for different sample plots (**Table 14**) in BNP for the period 2011-2014. Scatter plot between CASA NPP and field based NPP is depicted in **Figure 25**. There was a good agreement between both the data sets with coefficient of determination (R^2) 0.91, explaining 91% variability at 95% confidence level. The mean values of ground and simulated NPP are 6.65 Mg ha^{-1}year^{-1} and 7.28 Mg ha^{-1}year^{-1}, respectively. Mean NPP obtained from the field measurements was relatively lower than the CASA simulated NPP with the root-mean square error of 0.98 Mg ha^{-1}year^{-1}, which was 14.5% of the mean observed NPP over the region.

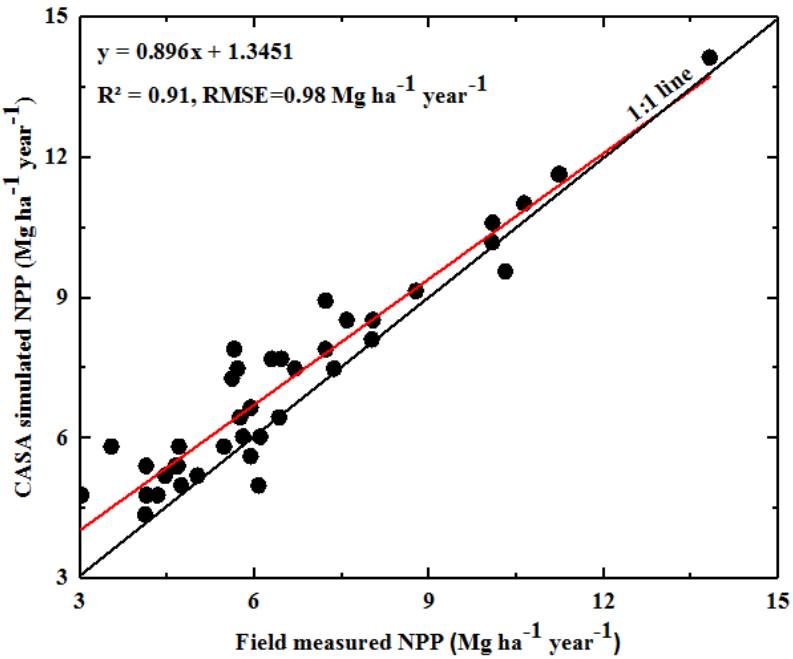

Figure 25: *Scatter plot describing the correlation between fields measured NPP and CASA derived NPP over BNP for the period 2011-2014.*

3.3 Madhav National Park

3.3.1 Field inventory: Among the ten plots (0.1 ha each) studied at tropical deciduous forest sites in MNP, 506 trees with DBH ≥ 3.18 cm were recorded. These trees belong to 18 tree species. Plot-wise distribution of tree types with their percentage contribution to the total tree population is presented in **Appendix 13**. Amongst these 18 species, seven species indicated stand density of >2%, whereas 11 species showed stand density of ≤ 2% of the total tree population. Out of all the recorded trees, trees of *Anogeissus pendula* (Kardhai) was found to be maximum with the presence of 149 trees, which was estimated to be 29.44% of the total tree density, followed by Khair (24.31%) and Salai (13.44%) respectively. Descriptive statistics of the sample plots studied in MNP is presented in **Table 18**. Among all the plots, Plot-7 contained the highest stand density with 87 trees, while Plot-4 indicated the lowest stand density with 14 trees. Analysis of the variance in tree height showed significant variations ($F=27.12$, $p<0.05$) across the sample plots. The tallest trees were observed in Plot-10 with a mean height of 11.23±3.29m, whereas shortest trees were observed in Plot-4 with an average height of 3.5±0.52m. Large variation in DBH was observed ($F=22.50$, $p<0.05$) between plots in the region. It was found to be more in Plot-6 with a mean DBH of 23.30±11.03m, whereas trees with poor DBH was observed in Plot-4 with an average DBH of 8.87±3.22m, respectively.

Table 18: *Descriptive statistics of different sample plots in MNP.*

Location	Plot	Tree density/0.1 ha	Average tree height (m) ±SD	Average DBH (cm)±SD
SR_Ammakunj beet	1	39	4.39±0.65	10.96±5.42
SR_Ammakunj beet	2	73	6.15±1.06	13.02±4.66
SR_Ammakunj beet	3	55	4.58±0.79	13.05±3.96
SR_Ammakunj beet	4	14	3.5±0.52	8.87±3.22
ER_Babanaua beat	5	29	9.33±2.66	20.73±8.31
CR_Dhamkan beat	6	28	7.14±2.63	23.30±11.03
CR_Dhamkan beat	7	87	3.83±0.93	9.03±2.17
CR_Eravan beat	8	56	8.08±2.24	15.50±5.89
NR_Bhurakha beat	9	58	4.54±1.26	11.89±5.56
SR_Kota beat	10	67	11.23±3.29	20.68±12.79

SR: South range; ER: East range; CR: Central range; NR: North range

Aboveground biomass (AGB): AGB was estimated using volumetric regression equations for the trees having DBH ≥ 3.18 cm. AGB estimation was carried out for each trees species of different classes in each sample plot for the period 2010-2014.

Per plot biomass (0.1ha) was determined by summing up the biomass of different individuals occurring in the plots. After calculating per plot biomass (kg/0.1ha), the total biomass was calculated in megagrams per hectare (Mg ha^{-1}), and these values were extrapolated to the hectare using Eq.2. Plot-wise biomass per hectare for the period 2010-2014 are presented in **Table 19**. A wide variation in AGB was observed between the plots, varying from 3 Mg ha^{-1} to 186 Mg ha^{-1}. Plot-10 holds the greatest biomass stock throughout the study period with an average biomass of 177.8±5.28 Mg ha^{-1}, ranging from 171.2 Mg ha^{-1} (2010) to 185.6 Mg ha^{-1} (2013). Least biomass storage was accounted throughout the study period in Plot-4 with an average biomass of 8.33±5.39 Mg ha^{-1}, varied from 2.95 Mg ha^{-1} (2010) to 14.76 Mg ha^{-1} (2013). Mean AGB across the plots was found to be highest in 2013 (185.67±49 Mg ha^{-1}), whereas the lowest AGB (171.2±48.6 Mg ha^{-1}) was observed in 2010. This inter-annual variation in AGB was attributed to variation in DBH, stand density, and percentage of trees showed increment in their growth. Plot-wise inter-annual variation in DBH with other attributes are presented in **Appendix 14**.

Table 19: *AGB for different sample plots in MNP for the period 2010-2014.*

		AGB (Mg ha^{-1})					
Location	Plot	2010	2011	2012	2013	2014	Mean±SD
SR_Ammakunj beet	1	17.16	18.85	20.98	32.96	27.29	23.45±6.56
SR_Ammakunj beet	2	40.04	42.86	47.61	55.24	51.66	47.48±6.21
SR_Ammakunj beet	3	27.83	29.32	32.51	41.62	39.83	34.22±6.2
SR_Ammakunj beet	4	2.95	4.60	5.91	14.76	13.43	8.33±5.39
ER_Babanaua beat	5	56.35	58.13	61.63	70.45	68.23	62.96±6.18
CR_Dhamkan beat	6	81.65	83.86	87.98	100.65	94.51	89.73±7.82
CR_Dhamkan beat	7	14.98	16.86	19.33	31.55	25.96	21.73±6.88
CR_Eravan beat	8	50.54	52.89	55.58	66.11	62.93	57.61±6.65
NR_Bhurakha beat	9	29.96	34.63	36.35	43.60	38.12	36.53±4.98
SR_Kota beat	10	171.20	175.58	178.35	185.67	178.60	177.88±5.28

Of the 10 plots, 98% of trees in Plot-1, while only 79% of the trees in Plot-10 were indicated increment in their growth (DBH), which were the highest and lowest among all the plots. About 80%-90% of trees in the remaining plots were exhibited increment in their growth. Maximum number of trees (91%) showed increment their growth in 2012, whereas only 81% of trees indicated increment in 2011. Rate of increment in DBH (cm $year^{-1}$) was another crucial biophysical parameter, where wide variation in AGB was observed due to its variation across the plots. Plots those covered with poor stand density showed large increment in DBH, while plots with high stand density

indicated poor increment in their DBH. Average increment in DBH across the plots varied from 0.91 cm year^{-1} to 0.28 cm year^{-1}. The highest increment was observed in Plot-4, where the plot was covered with lowest stand density (14 trees/0.1ha) among all the plots. Whereas the lowest increment in DBH was observed in Plot-10, where the plot covered relatively high stand density (67 trees/0.1ha) and dominated by single species, i.e., *Syzygium cumini***.** Though only 88% of trees showed increment in 2013, but mean increment in DBH was found to be highest in 2013 with an average increment of 0.53cm year^{-1}, whereas the highest number of trees (90%) showed increment in 2014 but their rate of increment in DBH was very poor with an average of 0.40cm year^{-1}. Relative deviation (RD%) in AGB across the study years is presented in **Appendix 15**. RD in AGB represented as $RD(\%)=100*((AGB_i-AGB_{2010})/AGB_{2010})$, where i represent AGB in 2011, 2012, 2013 and 2014, respectively. Though stand density and biomass stock was very less in Plot-4, but inter-annual change in biomass was very high among all the plots. Average biomass change in the plot was about 227% of its biomass in 2010. Whereas minimum change in AGB was observed in Plot-10 with 4.9%. RD across the plot was found to be highest in 2013 with an average of 83%, whereas the lowest change in AGB was observed in 2011 with a mean of 12%.

Field based NPP: Net primary productivity (NPP) of the tree species lying within the sample plots in MNP was estimated by dividing change in their AGB (ΔAGB) with time difference (Δt). More specifically, ΔAGB is the difference between current AGB (t2) and the back calculated AGB (t1). NPP value thus obtained was kg/0.1ha/year. After calculating NPP per plot, total NPP was calculated in megagrams per hectare per year (Mg ha^{-1} year^{-1}) using conversion factors given in Eq.2, and this value was extrapolated to the hectare. Plot-wise NPP for the study period 2011-2014 are presented in **Table 20**. There was a significant variation in NPP obtained across the plot for study period. Average NPP computed over the study period varied from 3.73±1.8 Mg ha^{-1} year^{-1} to 2.42±1.13 Mg ha^{-1} year^{-1}. Plot-6 had the highest mean NPP, while Plot-4 had the lowest NPP. Mixed forest with large increment in their DBH (0.41cm year^{-1}) played a crucial role to attain highest NPP in Plot-6. Though mean increment in DBH (0.91 cm year^{-1}) was maximum in Plot-4, but due to poor stand density (14 trees/0.1ha), plot was witnessed with the lowest NPP among all the plots. NPP values appeared to fluctuate across the plots from 2011 to 2014. Range of NPP was from 2.49±1.1 Mg ha^{-}

^{1} year^{-1} (2011) to 5.0±0.6 Mg ha^{-1} year^{-1} (2013) with an average of 3.2±1.2 Mg ha^{-1} year^{-1}.

Table 20: *Field based NPP for different sample plots in MNP for the period 2011-2014.*

		NPP (Mg ha^{-1} year^{-1})				
Location	Plot	2011	2012	2013	2014	Mean±SD
SR_Ammakunj beet	1	1.69	1.91	5.27	2.53	2.85±1.65
SR_Ammakunj beet	2	2.82	3.78	5.07	2.90	3.64±1.04
SR_Ammakunj beet	3	1.49	2.34	4.60	3.00	2.86±1.31
SR_Ammakunj beet	4	1.65	1.48	3.94	2.62	2.42±1.13
ER_Babanaua beat	5	1.78	2.64	4.70	2.97	3.02±1.23
CR_Dhamkan beat	6	2.21	3.17	6.33	3.21	3.73±1.8
CR_Dhamkan beat	7	1.88	2.18	5.52	2.75	3.08±1.67
CR_Eravan beat	8	2.35	2.52	5.19	3.10	3.29±1.31
NR_Bhurakha beat	9	4.67	3.20	4.55	2.04	3.61±1.24
SR_Kota beat	10	4.37	3.58	4.82	1.85	3.66±1.31

3.3.2. Climate variability

Based on daily values obtained from AMS tower, cumulated monthly rainfall, monthly average temperature and shortwave radiation (estimated from equation in **Figure 13**) were calculated and their characteristic seasonal pattern over MNP for the period 2011-2014 have been depicted in **Figure 26**. These figures illustrate that rainfall accumulated mainly between June and September. High rainfall values appeared from July to September. More than 92% of the total rainfall in the season was received during this period. Maximum rainfall seen in July, ranging from 228 mm (2013) to 336 mm (2012). Occasional winter rains occurred during December-February with the Northeast monsoon constituting 5% of the annual rainfall in the region. Number of rainy days (60 days, i.e. days with rainfall of 2.5 mm or more) was found to be very high in 2011, while minimum rainy days were observed in 2012 (24 days). Annual rainfall varied across the study period from 454 mm (2012) to 937 mm (2011) with an average of 725±198 mm. The region had received about 38% less rainfall in 2012 as compared to its mean annual rainfall. Seasonal temperature and radiation pattern over the region indicate that the pre-monsoon (March-May) season was very hot, with very high temperature and radiation values. Temperature during this period generally varied from 29 ^{o}C (March) to 38 ^{o}C (May). Consequently, radiation during the same period ranged from 405 Wm^{-2} to 698 Wm^{-2}. During September, there was a little rise in temperature and radiation values. Both the parameters fall rapidly from November, which lasts until

February. January was generally the coldest month with mean monthly temperature and radiation at 19 °C and 134 Wm^{-2}, respectively. No significant difference was observed in mean annual temperature and solar radiation received across the study period. Mean annual temperature ranged from 29.43 ^{o}C (2014) to 29.80 ^{o}C (2011) with an average of 29.59±0.14 ^{o}C. Mean annual solar radiation varied from 430 Wm^{-2} (2014) to 440 Wm^{-2} (2011) with an average radiation of 434±4 Wm^{-2}.

3.3.3 Satellite data analysis

Atmospheric correction: Atmospheric correction was performed for all the satellite images acquired over MNP for the study period. The analysis was carried out using Fast Line-of-sight Atmospheric Analysis of Spectral Hyper cubes (FLAASH) atmospheric correction module. To undertake a detailed atmospheric correction, aerosol optical depth (AOD) covering the date of satellite pass over the study region was obtained from the MODIS (MOD08_M3, 0.55 µm) global AOD data product. Characteristic temporal profile of AOD over MNP varied from 0.18 – 0.57. It was found to be lower in winter and higher in monsoon. Initial visibility (km) calculated from the AOD appeared to be maximum in winter months (49.8 km) and minimum in monsoon months with 13.61 km. **Figure 27a-b** depicts 28 October 2010 Landsat false colour composite before (TOA, uncorrected) and after atmospheric correction (corrected) over the study region. The improvement in contrast between various features with edges between features could be seen in the corrected image. **Figure 27c-d** shows the histograms of TOA reflectance and atmospherically corrected reflectance for Red and NIR bands of Landsat satellite data. Reduction in reflectance values and histograms shifting towards the origin were observed in red band after atmospheric correction, whereas the reflectance values in the NIR band increased after the atmospheric correction.

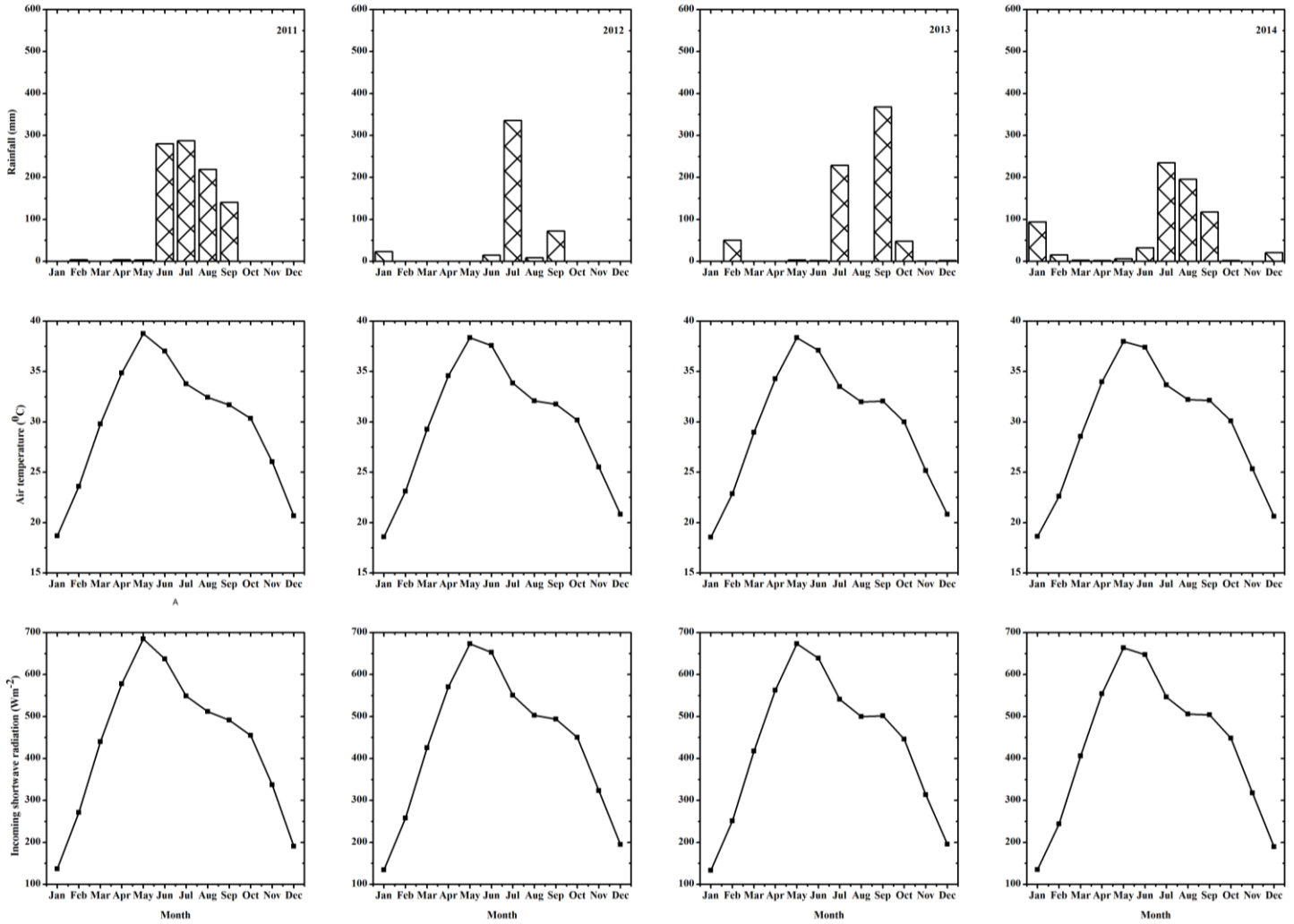

Figure 26: *Climate variability in MNP during the study period.*

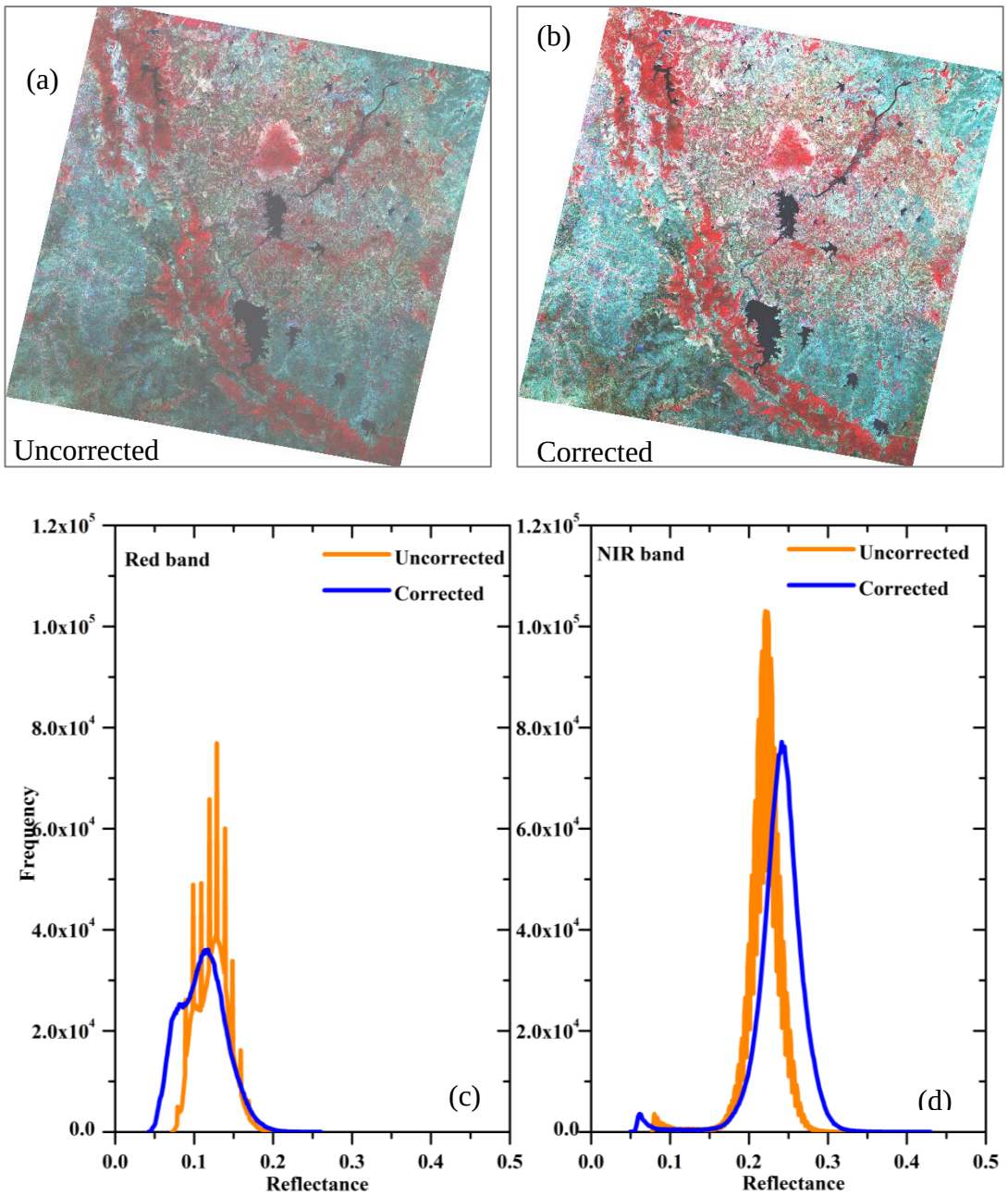

Figure 27: *Effect of atmospheric correction, a-b) uncorrected (TOA) and corrected Landsat scene, c-d) histograms of red and NIR band before and after atmospheric correction.*

MNP-LULC: Landsat based multi-temporal images representing three key phenological stages (start of senescence and leafless phase and full growth phase) of deciduous forests in MNP were used to generate landuse/landcover map of the region. Multi-date satellite images obtained over the region are depicted in **Figure 28**. Unsupervised classification scheme with more than 80 clusters were taken for image classification, of which eight LULC classes have been identified in the region. LULC map for MNP is shown **Figure 29** and statistics of the region generated from the classified

Figure 28: *Multi-date Landsat 5 TM satellite images coinciding with key phenological phases in MNP.*

output image is presented in **Table 21**. The table shows the spatial extent of land cover in square kilometre (km^2) and in percentages. Total geographical area of MNP estimated from satellite data was about 357.8 sq.km. Mixed forest dominated by Kardhai constitutes bulk of the total geographical area of the park. Around 29.88% of the total area belongs to the Mixed forest dominated by Kardhai with an area of 106.90 sq.km. Mixed forest dominated by Khair was covered with 93.47 sq.km (26.12%) followed by Mixed forest dominated by Salai with an area about 80.22 sq.km (22.42%). Grassland, Scrubland, Fallowland and Water bodies form the remaining portion of the park.

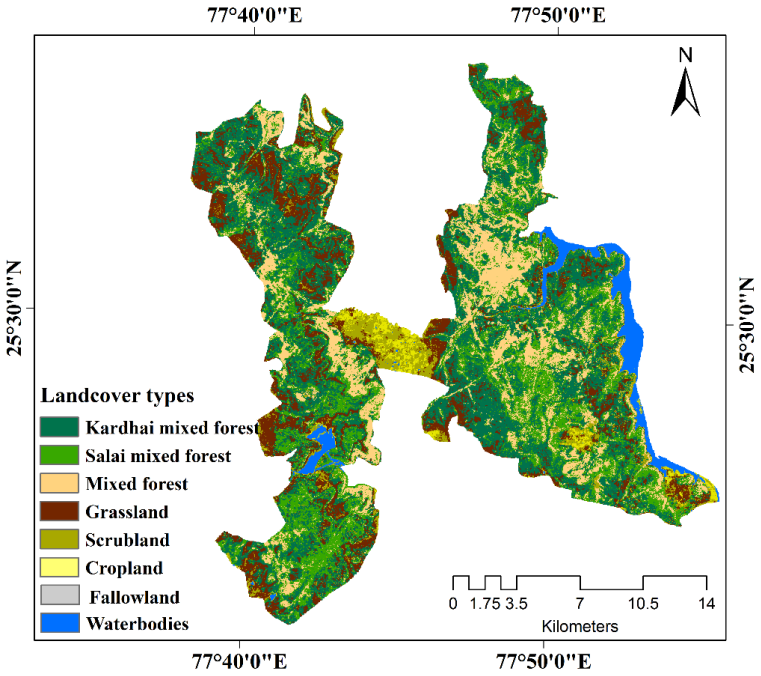

Figure 29: *Forest cover map of Madhav National Park.*

Table 21: *Distribution of forest types in MNP.*

Class code	Forest class	Area (Sq. km)	Percent of total area
1	Mixed forest dominated by Kardhai	106.90	29.88
2	Mixed forest dominated by Salai	80.22	22.42
3	Mixed forest dominated by Khair	93.47	26.12
4	Grassland	32.34	9.04
5	Cropland	3.87	1.08
6	Scrubland	25.23	7.05
7	Fallow land	1.77	0.49
8	Waterbodies	14.00	3.91
	Total	**357.80**	**100.00**

Accuracy Assessment of the classified image: Accuracy assessment was performed by comparing two sources of information (Jensen, 1996) one being the remote sensing based classified output images and other being the ground survey data (reference data). The reference data include biomass sample plots selected in the present study as well as ground control points taken during field survey especially conducted for verifying this satellite derived LULC map for MNP. Relationship between these two data sets results in an error matrix, which was used to determine overall accuracy of the classification. **Table 22** presented below illustrates the forest type wise Producer's and User accuracy achieved in the present study.

Table 22*: Classification accuracy assessment report for MNP.*

Class Code	Class name	Reference Totals	Classified Totals	Number Correct	Producers Accuracy (%)	Users Accuracy (%)
1	Mixed forest dominated by Kardhai	28	26	25	89.3	96.2
2	Mixed forest dominated by Salai	23	20	18	78.3	90.0
3	Mixed forest dominated by Khair	25	23	20	80.0	87.0
4	Grassland	11	9	9	81.8	100.0
5	Cropland	8	6	5	62.5	83.3
6	Scrubland	4	3	3	75.0	100.0
7	Fallow land	3	3	3	100.0	100.0
8	Waterbodies	3	3	3	100.0	100.0
	Total	**105**	**93**	**86**		

Overall accuracy=82%

Results showed that producer's accuracy varied between 62.5% and 100%. Fallowland and waterbodies indicated the highest accuracy with 100%, whereas cropland showed

the poor accuracy with 62.5%. Except cropland, all the classes show a user accuracy between 85% and 100%, while the relatively low accuracy was possessed by the cropland (83.3%). A measure of overall behaviour of the unsupervised (ISODATA) classification can be determined by the overall accuracy, which was the total percentage of pixels correctly classified. The unsupervised classification yielded an overall accuracy of 82% in MNP, indicating very high agreement with the ground truth.

CASA NPP modelling: Spatial and temporal variability of deciduous forest NPP in MNP was estimated using CASA ecosystem model based on multi-temporal Landsat images and meteorological data recorded at AMS towers for the period 2011-2014. CASA model simulates NPP in terms of carbon stock (MgC ha^{-1} $year^{-1}$), whereas field measured NPP obtained in this study were in biomass stock (Mg ha^{-1} $year^{-1}$). However, to make CASA NPP comparable with the field measured NPP, all the CASA NPP values were converted to biomass stock by assuming that the biomass stock was 2.08 times of the carbon sequestered by terrestrial vegetation (Sandra Brown and Lugo 1982; Ravindranath, Somashekhar, and Gadgil 1997). CASA simulated NPP values presented hereafter are in biomass stock (Mg ha^{-1} $year^{-1}$). **Figure 30** depicts CASA derived NPP over MNP from 2011 to 2014. Forests along the Sankya Sagar Lake and Atal Sagar Lake had higher NPP due to adequate water availability for their optimum growth. Whereas forests in North parts of the region had poor NPP due to sparse stand density. Using the landcover information (**Figure 29**), Kardhai mixed forest, Salai mixed forest and mixed forest were distinguished as predominant landcover types in the region. Average NPP of the four years of these forest types varied widely as value by mixed forest (5.78 Mg ha^{-1} $year^{-1}$) > Kardhai mixed forest (3.78 Mg ha^{-1} $year^{-1}$) > Salai mixed forest (3.16 Mg ha^{-1} $year^{-1}$). NPP was found to be higher in forests of Eastern regions, whereas NPP was appeared to be lower in Western parts of the region. To understand temporal variation of NPP over the study period, NPP values of five predominant forest types with the temporal change was made. It indicates that NPP varied little with the temporal change except that NPP value of all forest types was lower in 2012 than that in any other years. CASA simulated NPP obtained for different sample plots in MNP for the study period 2011-2014 is presented in **Table 23**. Wide variation in simulated NPP (1.73 Mg ha^{-1} $year^{-1}$ to 6.24 Mg ha^{-1} $year^{-1}$) between the plots was because of marked variations in species composition, stand density, and their canopy spread.

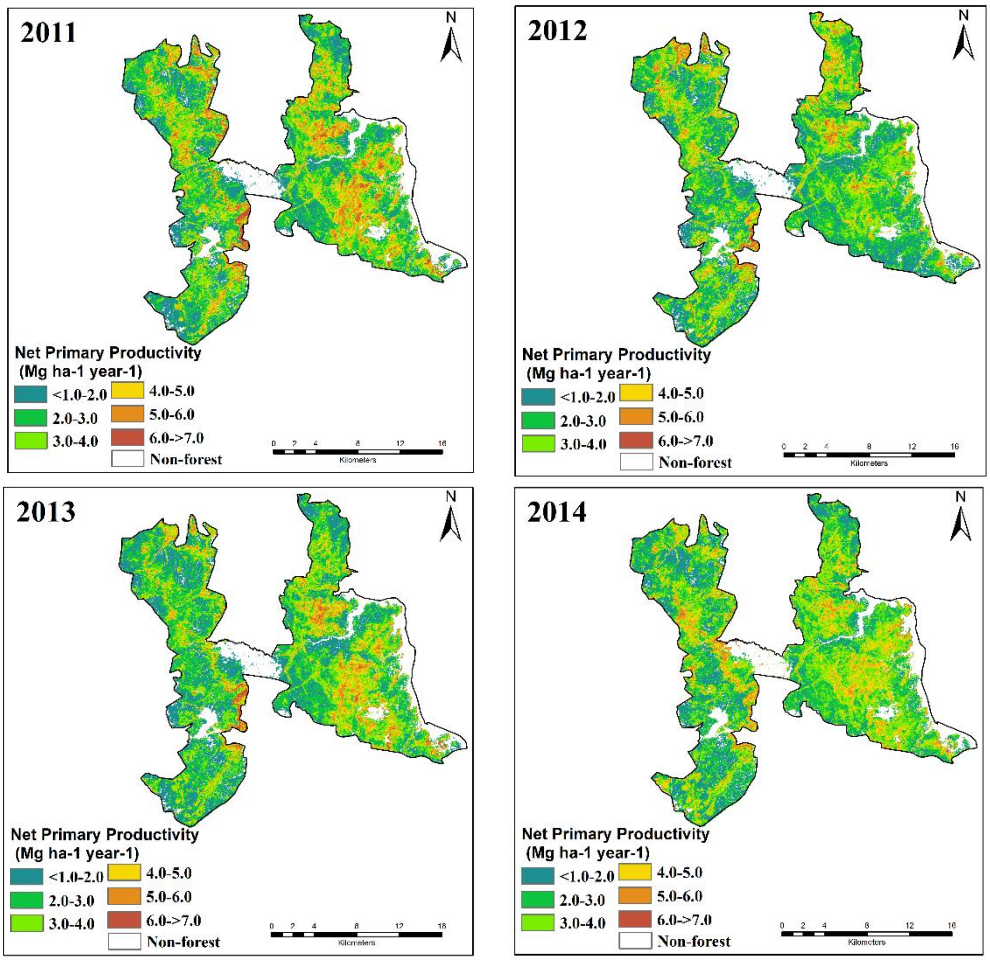

Figure 30: *Spatial variability of NPP over MNP for the period 2011-2014.*

High NPP was found concentrated in Plot-6 (NPP averaged across the study period, 5.22±2.0 Mg ha^{-1} $year^{-1}$) which was attributed to mixed forest composition with dense stand density. The lowest NPP was associated with Plot-4 (2.72±1.08 Mg ha^{-1} $year^{-1}$) due to sparse stand density and their poor growth. NPP averaged across the plots was found to be highest in 2013 (5.5±0.62 Mg ha^{-1} $year^{-1}$), while the lowest NPP (2.87±0.62 Mg ha^{-1} $year^{-1}$) was appeared in 2014 with an average NPP across the study period was about 3.7±0.2 Mg ha^{-1} $year^{-1}$.

CASA-NPP validation: Dry deciduous forest NPP simulated from the CASA ecosystem model was compared with the field measured NPP obtained for different sample plots in MNP for the period 2011-2014. Scatter plot between field based NPP and CASA NPP are depicted in **Figure 31**. There was a good agreement between both the data sets with coefficient of determination (R^2) 0.94, explaining

94% variability at 95% confidence level. The mean values of field and simulated NPP are 3.22 Mg $ha^{-1}year^{-1}$ and 3.71 Mg $ha^{-1}year^{-1}$, respectively.

Table 23: *CASA simulated deciduous forest NPP for different sample plots in MNP for the period 2011-2014.*

		NPP (Mg ha^{-1} $year^{-1}$)				
Location	Plot	2011	2012	2013	2014	Mean±SD
SR_Ammakunj beet	1	2.62	2.70	5.68	2.68	3.42±1.5
SR_Ammakunj beet	2	3.39	3.97	5.66	2.95	3.99±1.19
SR_Ammakunj beet	3	2.04	3.39	5.26	3.14	3.46±1.34
SR_Ammakunj beet	4	2.14	1.73	4.18	2.81	2.71±1.07
ER_Babanaua beat	5	2.27	3.16	5.24	3.16	3.46±1.26
CR_Dhamkan beat	6	3.12	4.04	6.26	3.85	4.32±1.36
CR_Dhamkan beat	7	2.70	2.91	5.80	2.93	3.59±1.48
CR_Eravan beat	8	3.47	3.35	5.87	3.18	3.97±1.27
NR_Bhurakha beat	9	4.87	3.47	5.49	2.10	3.98±1.51
SR_Kota beat	10	5.32	4.01	5.43	1.89	4.17±1.65

Mean NPP estimated by CASA model was relatively higher than the field measured NPP with the root-mean square error (RMSE) of 0.59 Mg $ha^{-1}year^{-1}$, which is 18% of the mean field measured NPP.

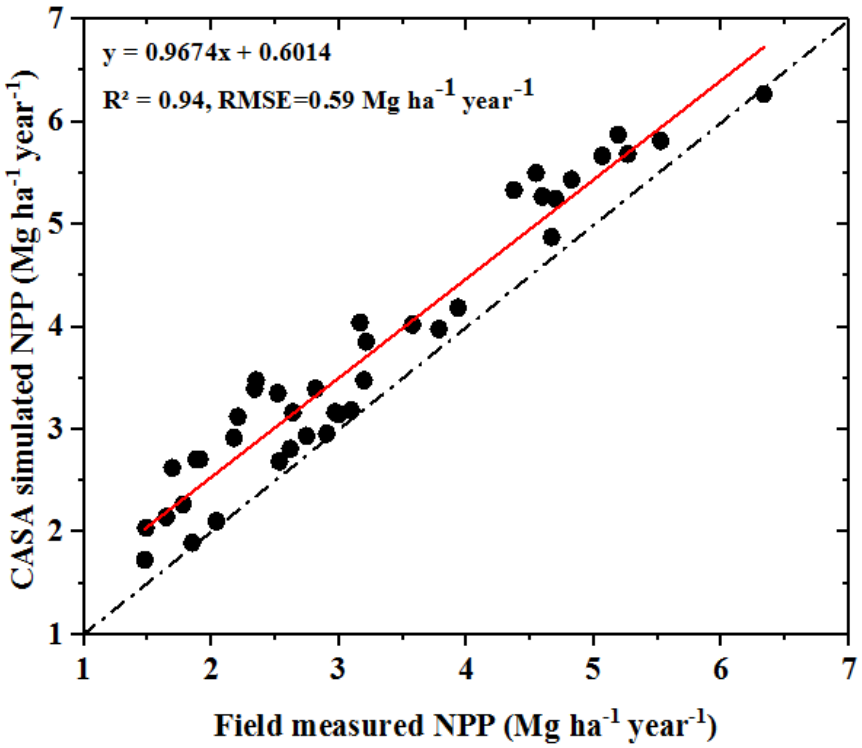

Figure 31: *Scatter plot describing the correlation between fields measured NPP and CASA derived NPP over MNP for the period 2011-2014.*

3.4 NPP and climate associations on a regional scale

An assessment was made in this analysis to determine relation between deciduous forest NPP and different climatic factors in KNP, BNP and MNP for the period 2011-2014. NPP simulated by CASA ecosystem model and different climatic parameters obtained from AMS towers were used for the analysis. Scatter plot between NPP and cumulated annual rainfall obtained for KNP, BNP and MNP is depicted in **Figure 32a**. Significant positive correlation was observed between both the parameters with coefficient of correlation (r) 0.88, which implies that 88% of NPP variability in these regions was governed by rainfall. Generally, the graph can be grouped in to three categories (low, medium and high). Low (low rainfall and low NPP) was associated with MNP; medium was related with BNP, whereas high was linked with KNP. Some of the points were mixed with their subsequent or preceding group due to change in their characteristic rainfall and NPP pattern. For instant, one of the points in MNP had shifted with its subsequent group (BNP) due to high rainfall in 2013. MNP had received 31% more rainfall in 2013 when compared to its mean annual rainfall, however forests in the region had sequestered 48% more NPP (5.5 Mg ha^{-1} $year^{-1}$) compared to its mean NPP (3.7 Mg ha^{-1} $year^{-1}$). Contrastingly, two points of KNP had shifted with their preceding group (BNP) due to comparatively low rainfall in 2013 and 2014, where forests had sequestered considerably low NPP in both the years. Correlation of NPP with mean annual temperature and radiation is showed in **Figure 32b-c**. Negative correlation was observed between both the parameters (r=0.37). Low NPP and high temperature was related to MNP, followed by high NPP and moderately low temperature was associated to KNP, whereas moderately low NPP and low temperature was linked to BNP. Since radiation was modelled using temperature, similar results were observed with radiation. Altogether, it is evident from the **Figure 32** that MNP consistently had low NPP during the study period was due to low rainfall, high temperature and high radiation. Relatively high NPP in BNP than MNP was due to moderately high rainfall and comparatively low temperature and low radiation, followed by high NPP in KNP was due to high rainfall and high temperature and high radiation.

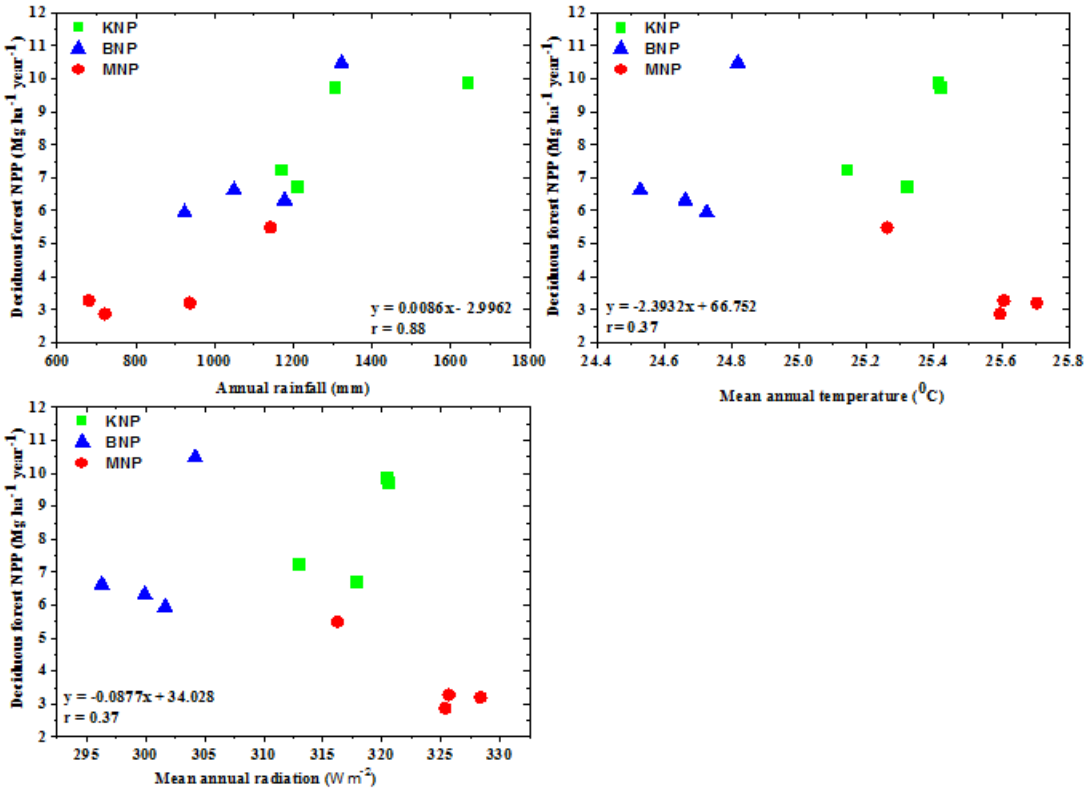

Figure 32: *Relation between NPP and different climate factors obtained over KNP, BNP and MNP for the period 2011-2014.*